Neutron Stars & Gravitational Waves

Kostas Kokkotas[1] & **Christian Krüger**[1,2]

1-Theoretical Astrophysics, University of Tübingen

2-Department of Physics, University of New Hampshire

The Many Faces of Neutron Stars

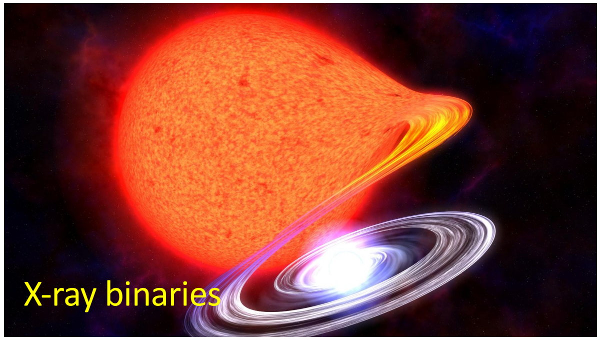

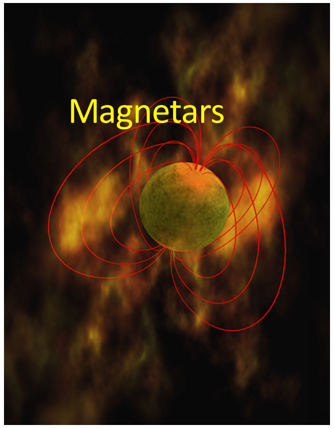

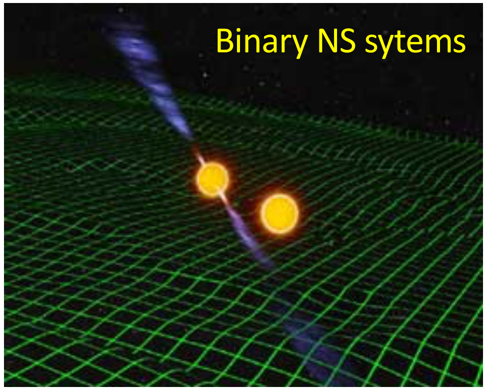

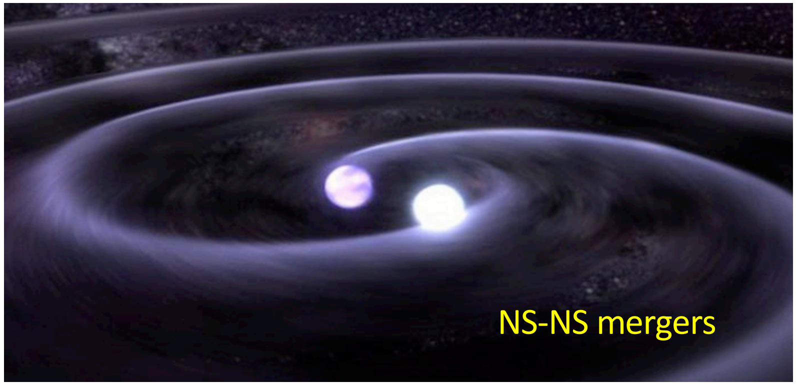

Typical masses ~1.2-2 $M_\odot$
Typical Radius ~9-14 km

Neutron Stars: Mass vs Radius

Static Models

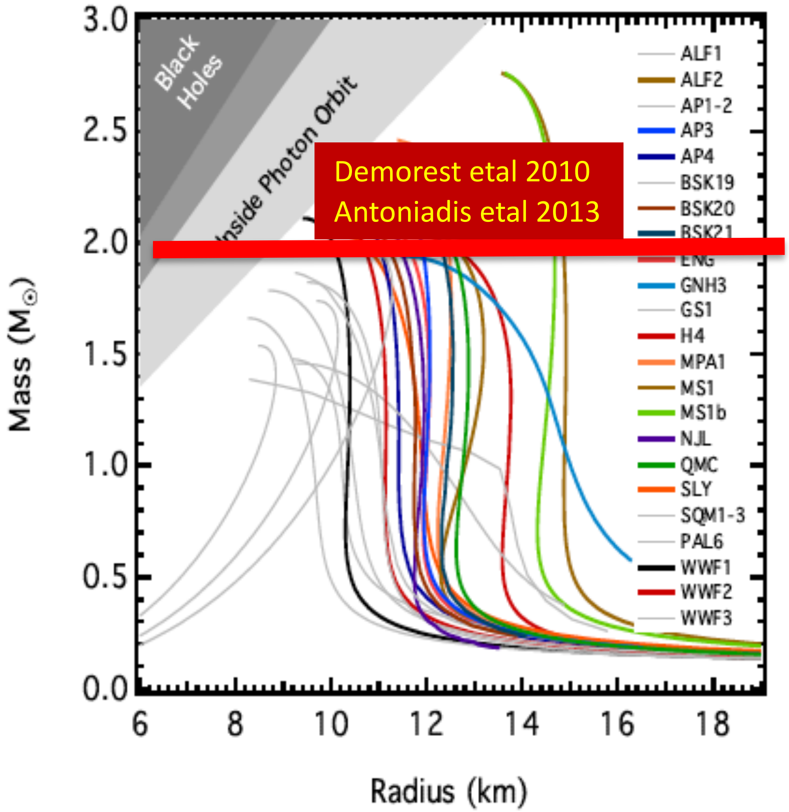

Özel & Freire (2016)

Rotating Models

supramassive

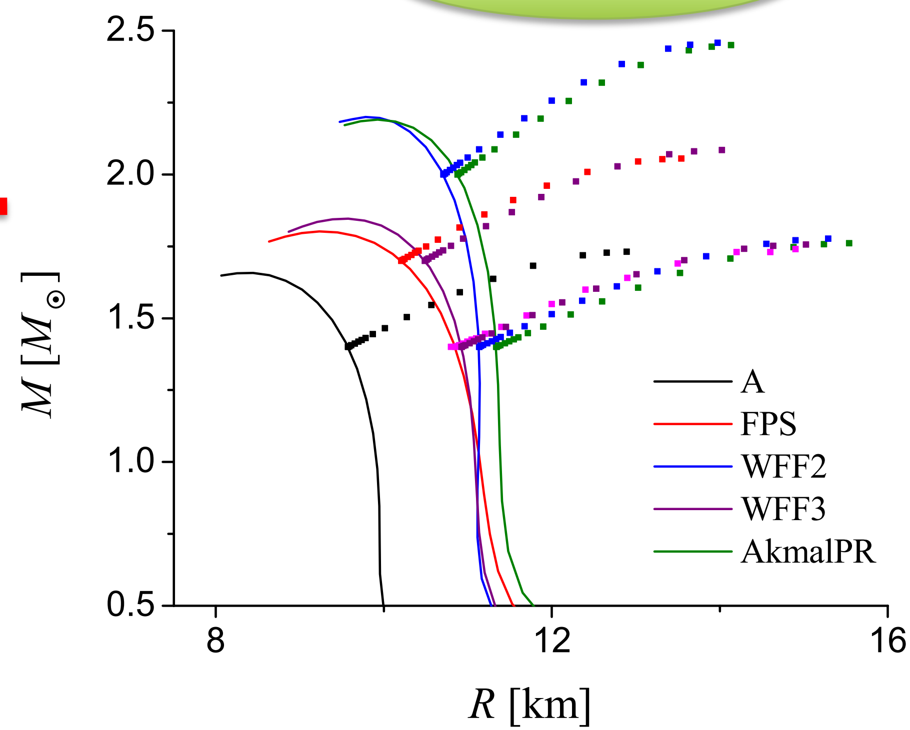

$$M_{max} \simeq 1.2\ M_{TOV}$$

Constraints on Neutron Star Radius
GW observations

Main methods in EM spectrum

- **Thermonuclear X-ray bursts (photospheric radius expansion)**
- **Burst oscillations (rotationally modulated waveform)**
- **Fits of thermal spectra to cooling neutron stars**
- **khZ QPOs in accretion disks around neutron stars**
- **Pericenter precession in relativistic binaries (double pulsar J0737)**

Main methods in GW spectrum

- **Tidal effects on waveform during inspiral phase of NS-NS mergers**
- **Tidal disruption in BH-NS mergers**
- **Oscillations in (early & late) post-merger phase**
- **Oscillation in the post-collapse phase**

Neutron Stars & "universal relations"

Need for relations between the "observables" and the "fundamentals" of NS physics

Average Density	$\bar{\rho} \sim M / R^3$	
Compactness	$z \sim M / R$	$\eta = \sqrt{M^3 / I}$
Moment of Inertia	$I \sim MR^2$	$I \sim J / \Omega$
Quadrupole Moment	$Q \sim R^5 \Omega^2$	
Tidal Love Numbers	$\lambda \sim I^2 Q$	

I-Love-Q relations

EOS independent relations were derived by **Yagi & Yunes(2013)** for non-magnetized stars in the slow-rotation and small tidal deformation approximations.

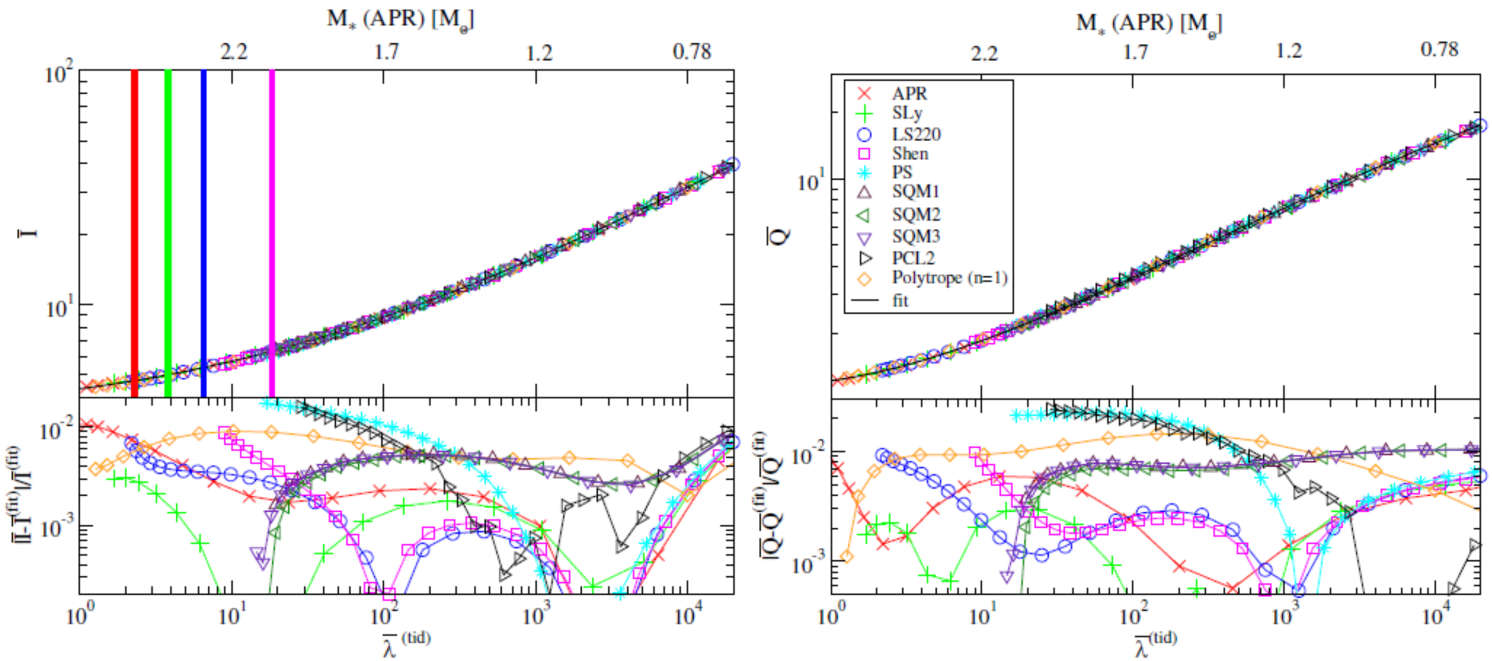

… the relations proved to be valid (*with appropriate normalizations*) even for *fast rotating* and *magnetized* stars

Latest developments: Yagi-Yunes arXiv:1601.02171 & arXiv:1608.06187

Oscillations & Instabilities

The most promising strategy for constraining the physics of neutron stars involves observing their "ringing" (oscillation modes)

- **f-mode :** scales with average density
- **p-modes:** probes the sound speed through out the star
- **g-modes :** sensitive to thermal/composition gradients
- **w-modes:** oscillations of spacetime itself.
- **s-modes:** Shear waves in the crust
- **Alfvèn modes:** due to magnetic field
- **i-modes:** inertial modes associated with rotation (r-mode)

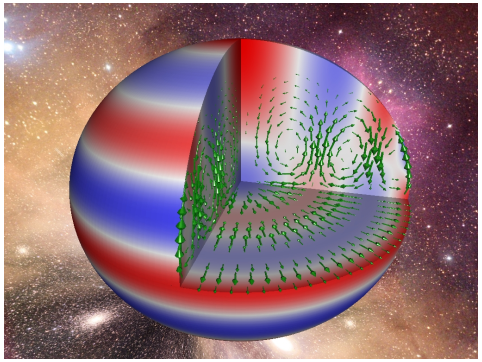

Typically **SMALL AMPLITUDE** oscillations –> weak emission of GWs
UNLESS
they become **unstable due to rotation** (r-mode & f-mode)

$l = 2, m = 2$

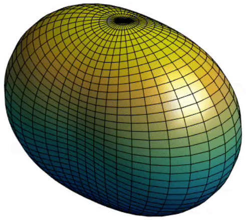

$l = 3, m = 3$

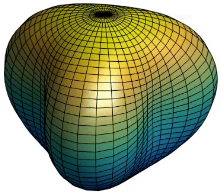

$l = 4, m = 4$

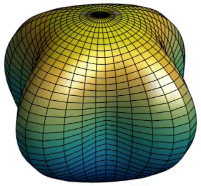

Oscillations & Instabilities

p-modes: main restoring force is the **pressure** (**f-mode**) ***(>1.5 kHz)***

$$\sigma \approx \sqrt{\frac{GM}{R^3}}$$

Inertial modes: (r-modes) main restoring force is the **Coriolis force**

$$\sigma \approx \Omega$$

w-modes: pure **space-time modes** (only in GR) ***(>5kHz)***

$$\sigma \approx \frac{1}{R}\left(\frac{GM}{Rc^2}\right)$$

Torsional modes (t-modes) ***(>20 Hz)*** shear deformations.
Restoring force, the weak Coulomb force of the crystal ions.

$$\sigma \approx \frac{v_S}{R} \sim 16\ \ell\ \mathrm{Hz}$$

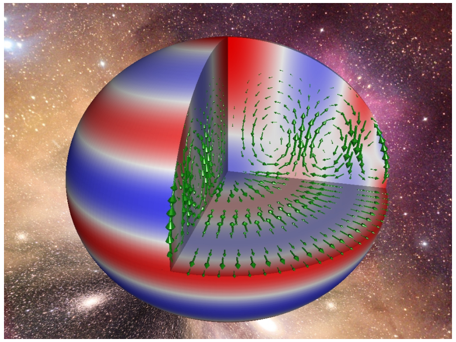

... and many more

shear, g-, Alfven, interface, … modes

Gravitational Wave Asteroseismology

Gravitational Wave Asteroseismology : Andersson-Kokkotas 96+

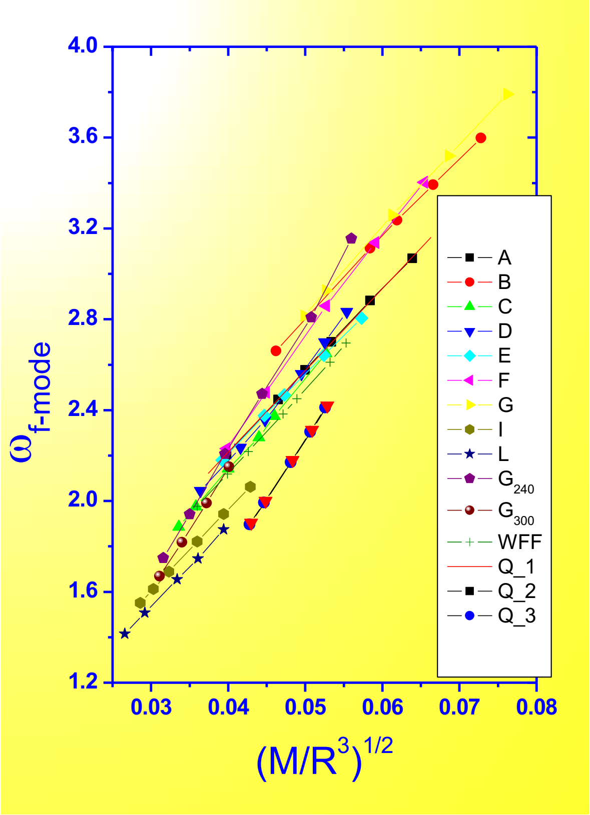

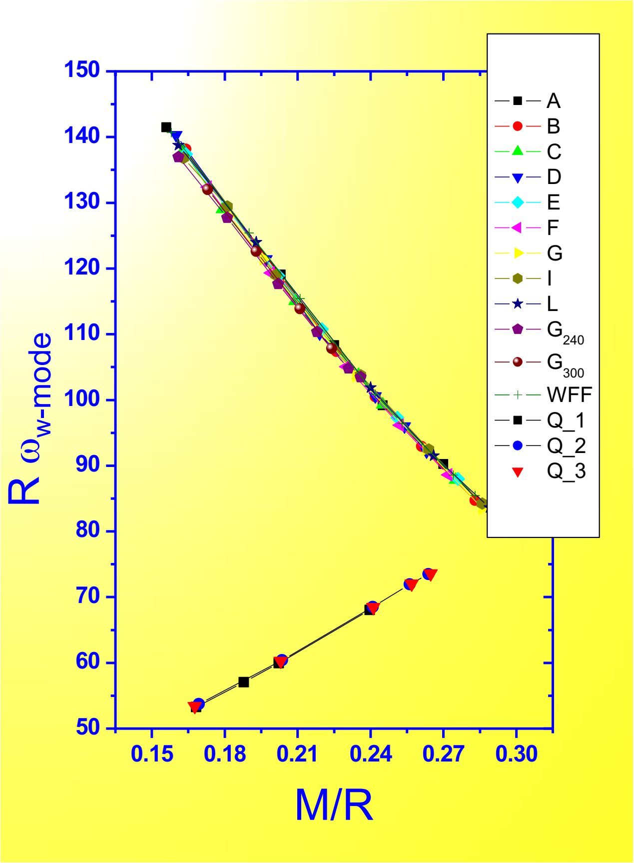

Binary Neutron Star Mergers
the standard scenario

The GW signal can be divided into **three distinct phases**

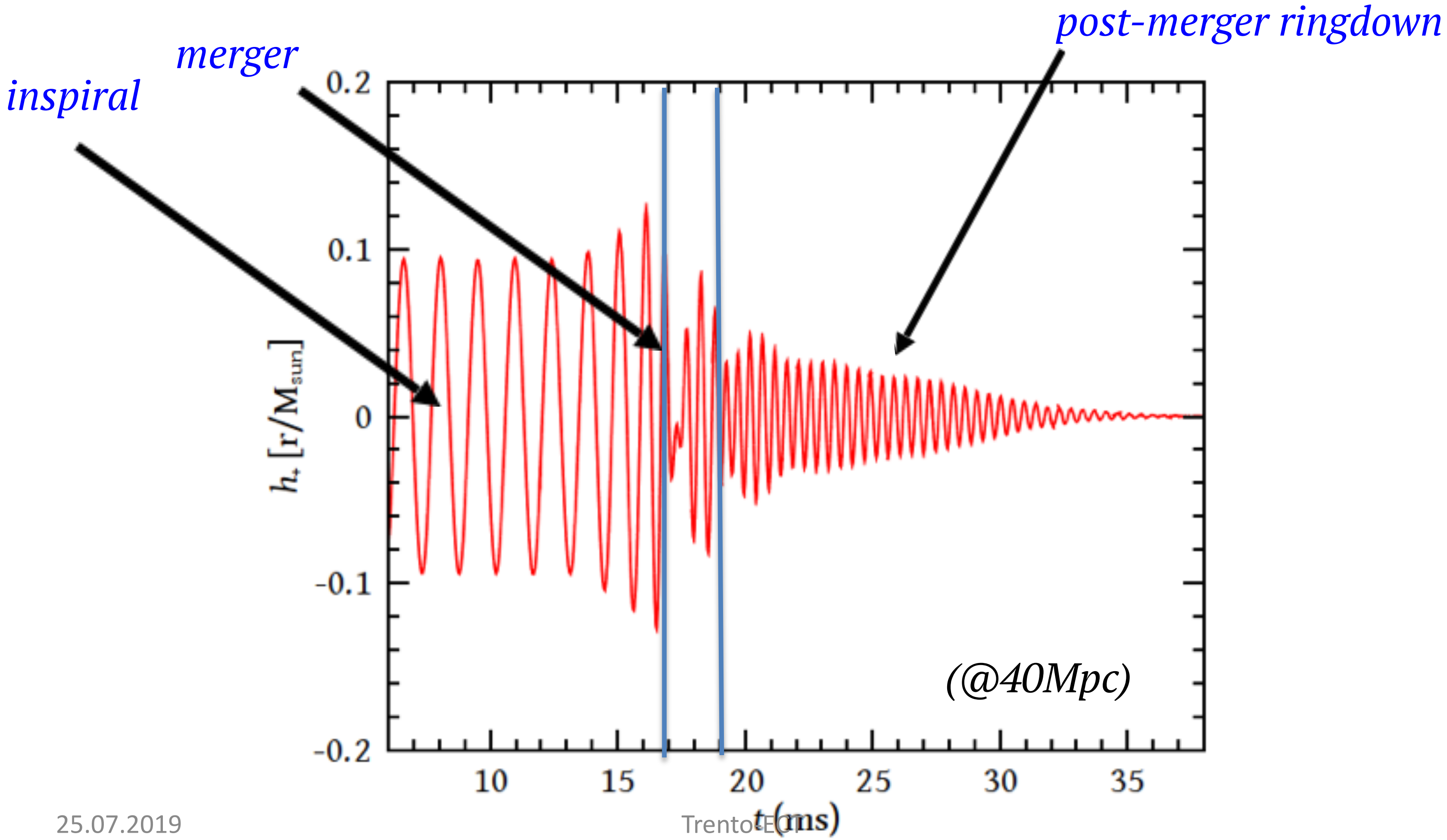

Binary Neutron Star Mergers

the post-Merger scenario

I. Direct collapse to BH if

$$M_{TOT} > M_{max}(\Omega)$$

II. Formation of an "unstable" NS if

$$M_{max}(\Omega) > M_{TOT} > M_{max}$$

III. Formation of a "stable" NS if

$$M_{TOT} < M_{max}(\Omega)$$

- NS-NS mergers will produce:
  - ~40% prompt BHS
  - ~30% supramassive NS -> BH
  - ~30% Stable NS

Gao, Zhang, Lü 2016

- Initial spin near breakup limit ~1ms

Differential rotation/turbulence -->

strongly twisted internal field $E_B \geq 10^{50} erg$

e.g. Rosswog etal (2003), Rezzolla etal 2011, Kiuchi etal 2012, Giacomazzo & Perna 2013, Giacomazzo etal 2015, Kyotoku etal 2015,…

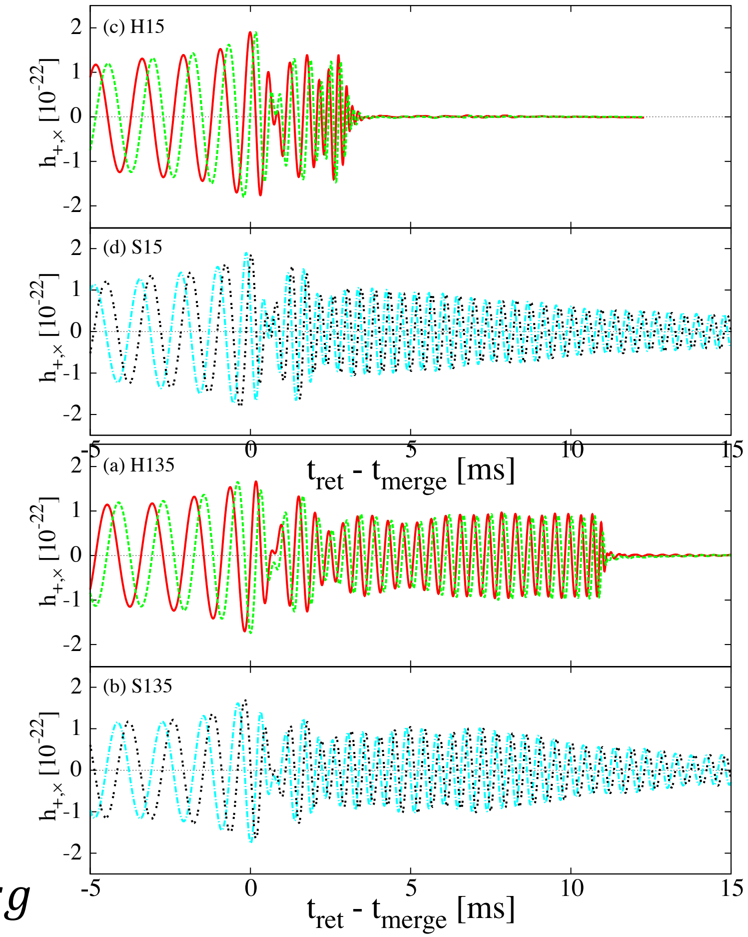

Kiuchi, Sekiguchi, Kyutoku, Shibata 2012

Binary Neutron Star Mergers
Tidal Interaction

Tidal interactions affect the last part of the inspiral, modifying the orbital motion and the GW emission.

Kokkotas-Schaefer MNRAS 1995

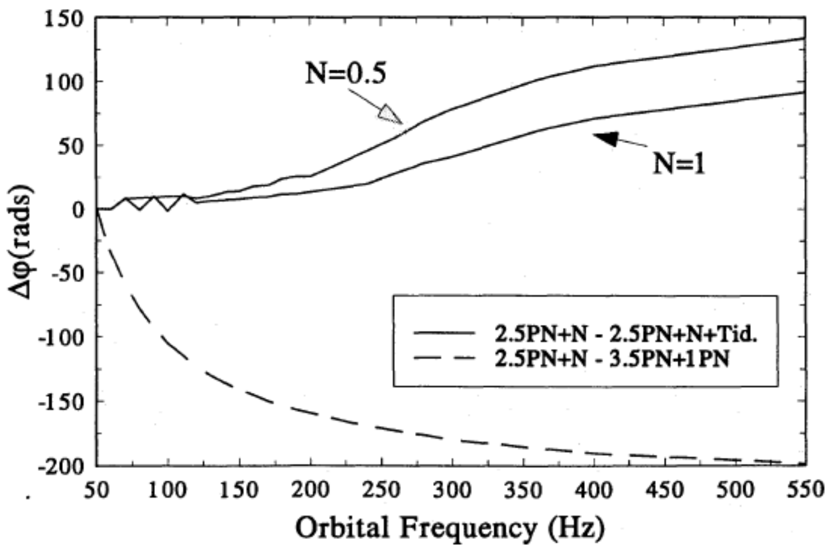

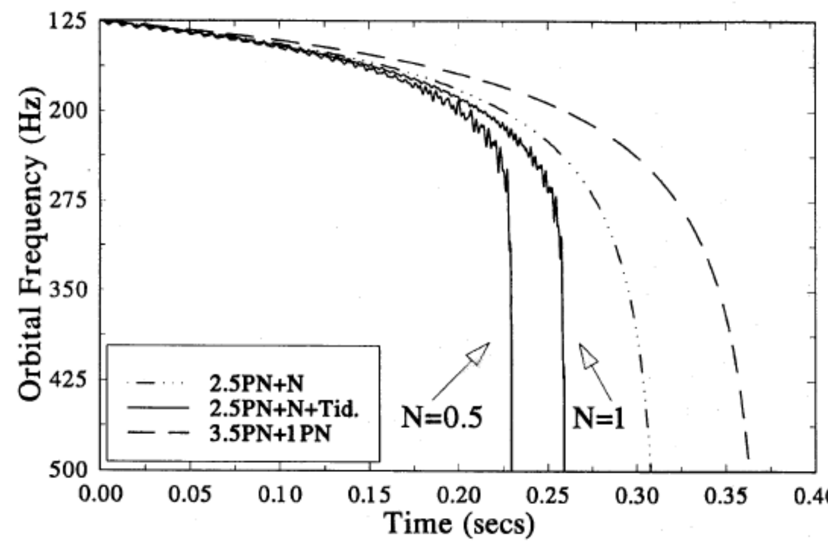

Bildsten-Cutler 1992
Kokkotas-Schaefer 1993-5
Lai et al 1993,1994
Shibata 1994
Flanagan 1998
Ho-Lai 1999
…

Binary Neutron Star Mergers
Tidal Interaction

Tidal interactions affect the last part of the inspiral, modifying the orbital motion and the GW emission.

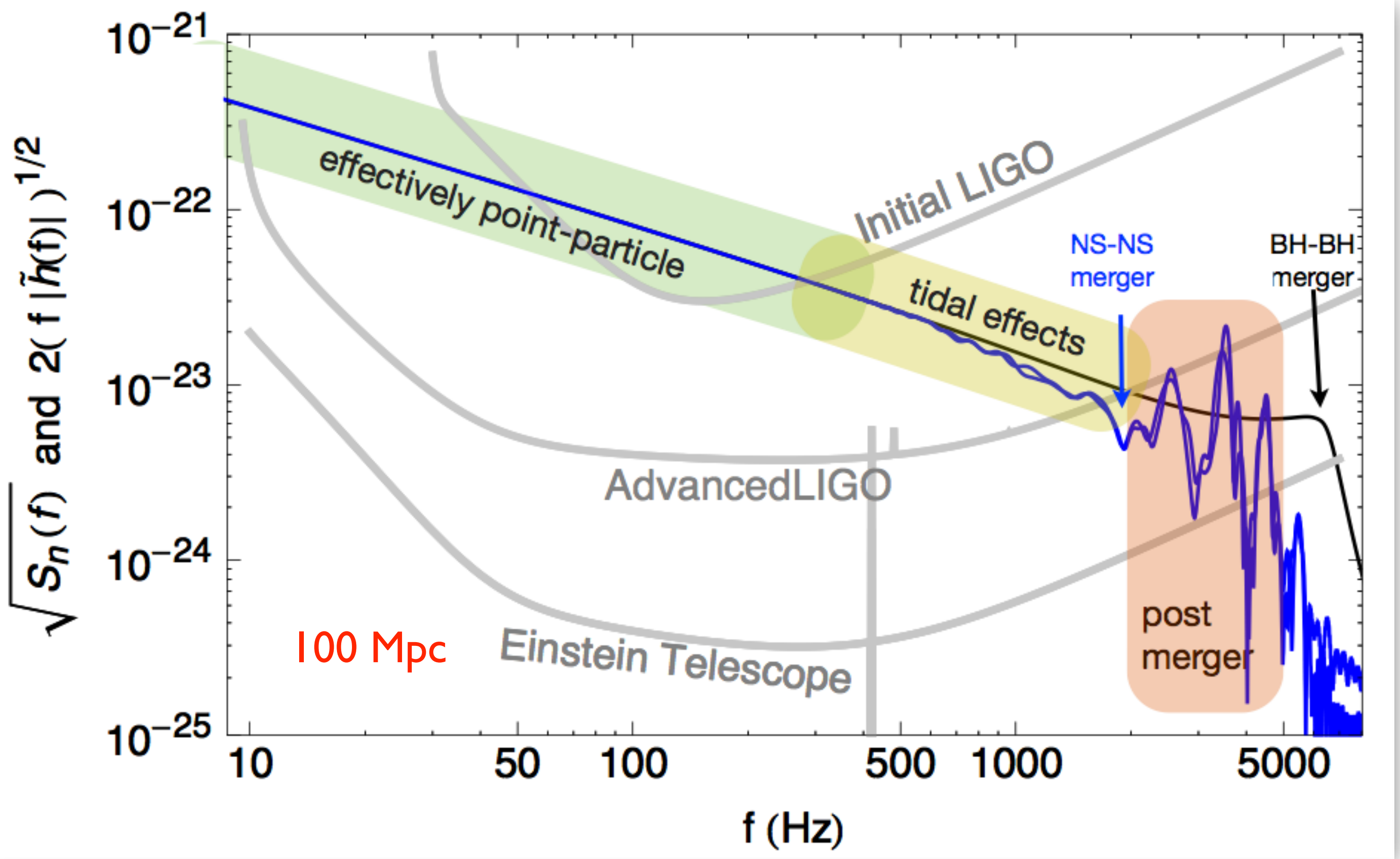

courtesy of Jocelyn Read

Binary Neutron Star Mergers
Tidal Love numbers

The last part of the inspiral signal carries the imprint of the quadrupole tidal deformability

$$\lambda = -\frac{Q_{ij}}{E_{ij}} = \frac{2}{3} k_2 R^5$$

Read et al. (2013), Hotozaka et al (2013)…

k_2 : tidal Love number

$$\Lambda \equiv \frac{2}{3} k_2 \left(\frac{R}{M} \right)^5$$

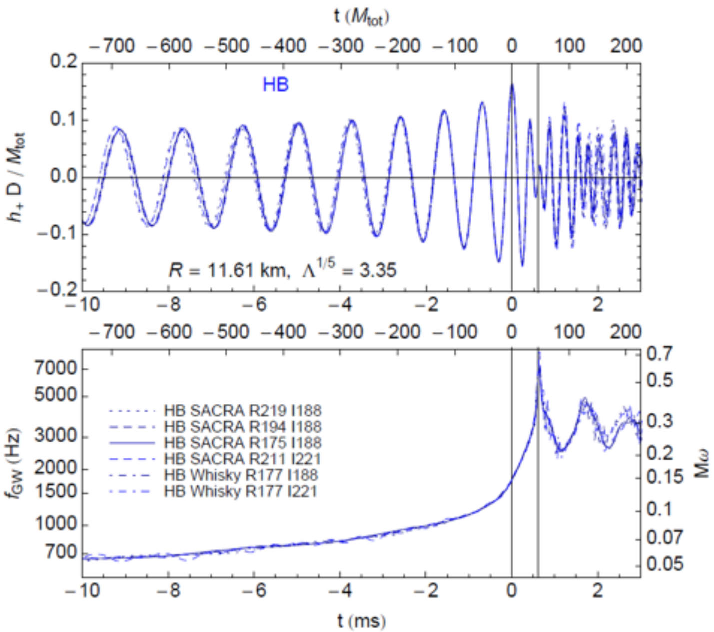

The leading tidal contribution to the phase evolution is a combination of the two tidal parameters. It is of 5PN order

$$\tilde{\Lambda} = \frac{16}{13} \frac{(m_1 + 12 m_2) m_1^4 \Lambda_1 + (m_2 + 12 m_1) m_2^4 \Lambda_2}{(m_1 + m_2)^5}$$

Measurements of M_{NS} and Λ would be helpful to constrain the NS EOS

With aLIGO

$\frac{\Delta R}{R} \sim 10\%$ at 100Mpc

Binary Neutron Star Mergers
Tidal Interaction

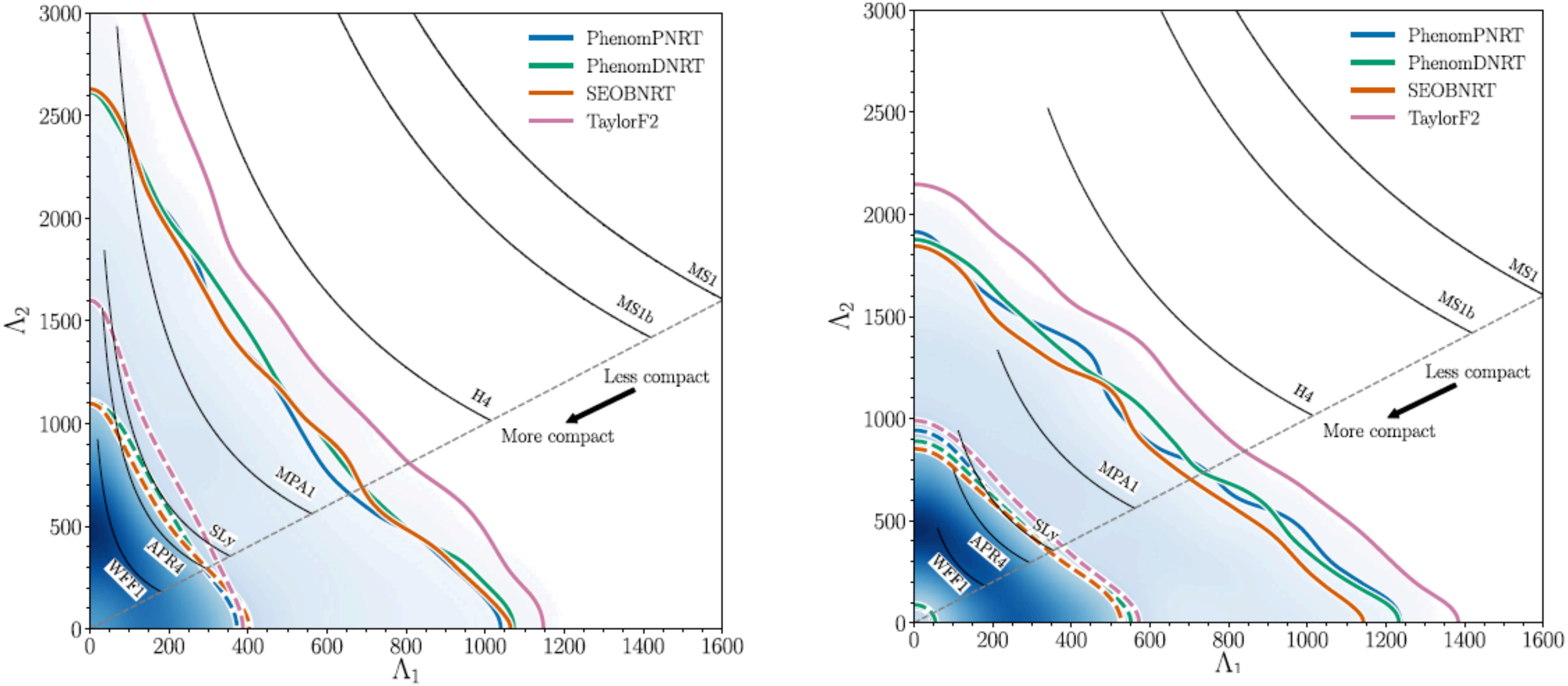

Probability density for the tidal deformability parameters of the *high spin* and *low spin* components inferred from the detected signals using the post-Newtonian model.

Equation of State:
Constraints from GW170817 (Bauswein etal)

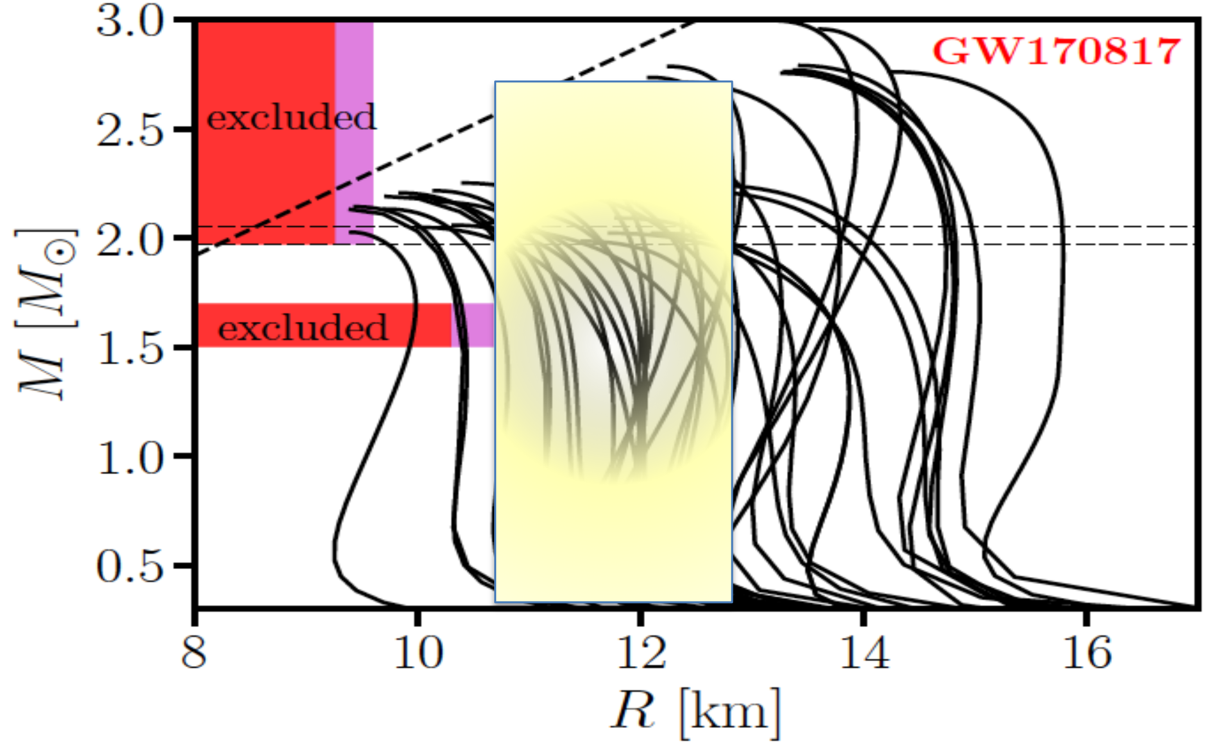

Figure 2. Mass-radius relations of different EoSs with very conservative (red area) and "realistic" (cyan area) constraints of this work for $R_{1.6}$ and R_{max}. Horizontal lines display the limit by Antoniadis & et al. (2013). The dashed line shows the causality limit.

Equation of State:
Constraints from X-ray binaries / bursts

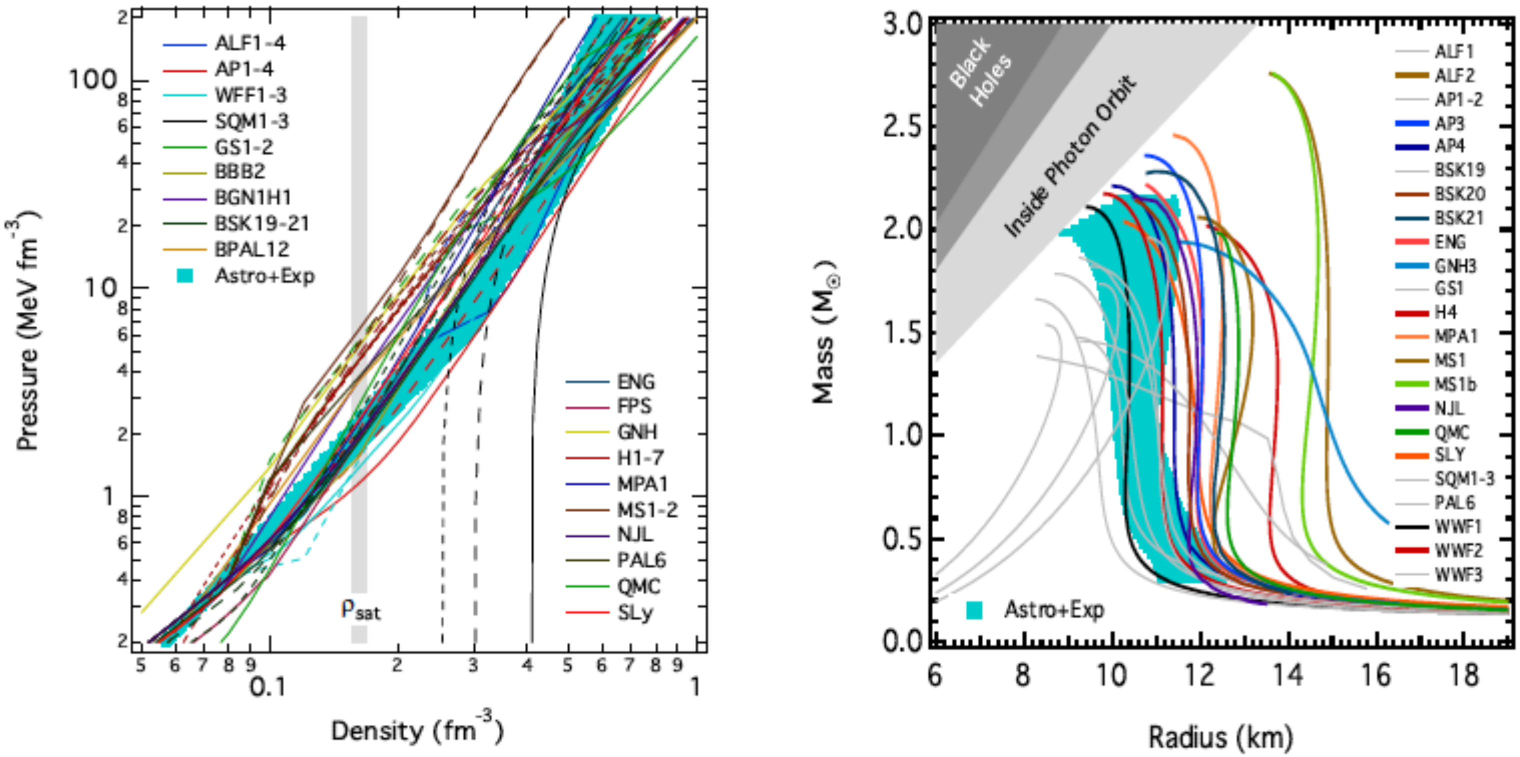

Figure 10

The astrophysically inferred (left) EoS and (right) mass-radius relation corresponding to the most likely triplets of pressures that agree with all of the neutron star radius and low energy nucleon-nucleon scattering data and allow for a $M > 1.97\ M_\odot$ neutron star mass. The light blue bands show the range of pressures and the mass-radius relations that correspond to the region of the (P_1, P_2, P_3) parameter space in which the likelihood is within e^{-1} of its highest value. Around $1.5\ M_\odot$, this inferred EoS predicts radii between 9.9 – 11.2 km.

Özel & Freire (2016)

Chandra & Kip in the 60-70s

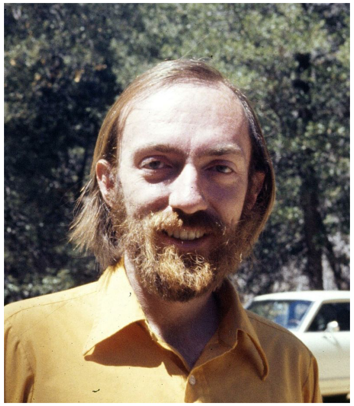

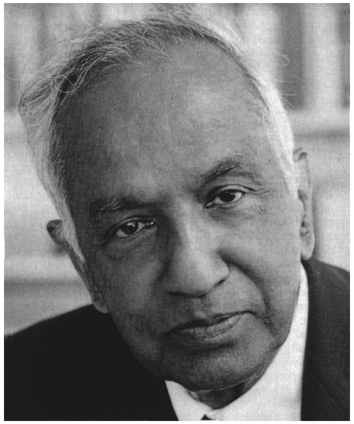

Together with

- Campollataro, A.
- Ipser, Jim
- Price, Richard
- Hartle, James B.
- Schutz, Bernard F.
- Detweiler S.
- Lindblom L.

Together with:

- Lebovitz Norman R.
- Tooper, Robert F.
- Nutku, Yavuz
- Esposito, Paul F.
- Friedman, J. L.

Study of nearly everything:

- Radial pulsations
- Non-radial Pulsations
- Emission of Gravitational Waves
- Slow-Rotation Approximation

Studies of Stability of Relativistic Stars/ellipsoids

- Post-Newtonian equilibria and Dynamics (up to 2.5 PN order)
- The first hints of the CFS secular instability

The work till now -I

The "CFS" Instability : Chandrasekhar – Friedman – Schutz 70+
Ergoregion Instability: Friedman, Schutz, Comins 70+
Systematic studies of stability properties of rotating stars and of CFS instability Friedman – Ipser – Parker – Lindblom 80+

Spacetime (w-) modes: Kokkotas-Schutz 1986-90+
Gravitational Wave Asteroseismology : Andersson-KK 90+
R-mode instability : Andersson; Friedman – Morsink 90+

ALL THESE STUDIES WERE DONE FOR:

- **Non-Rotating**
- **Slowly Rotating Stars**

Equilibrium configurations of fast rotating GR stars
Hachisu-Komatsu-Eriguchi (1988) more advanced codes later (Cook, Shapiro, Stergioulas, Friedman) 90+

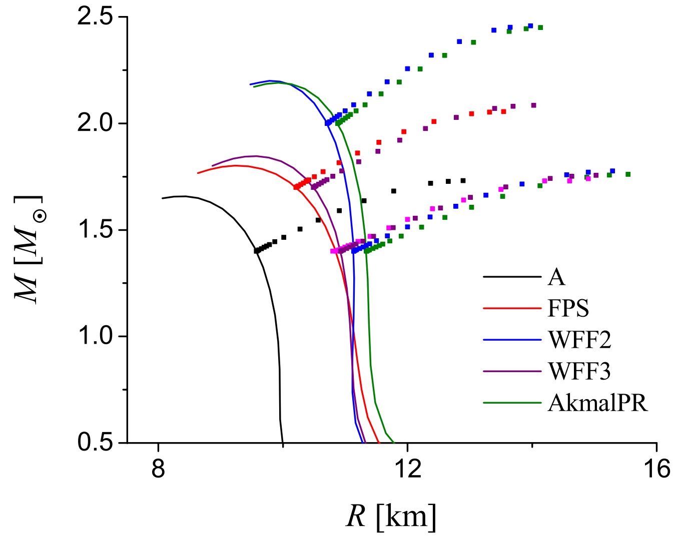

The work till now -II

Gravitational Wave Asteroseismology : Andersson-KK 96+

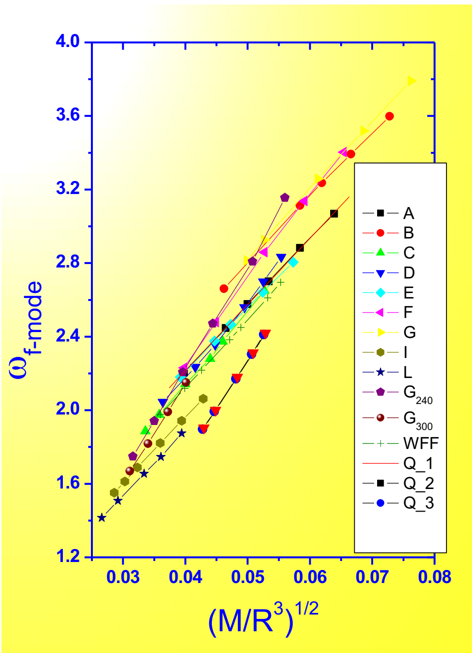

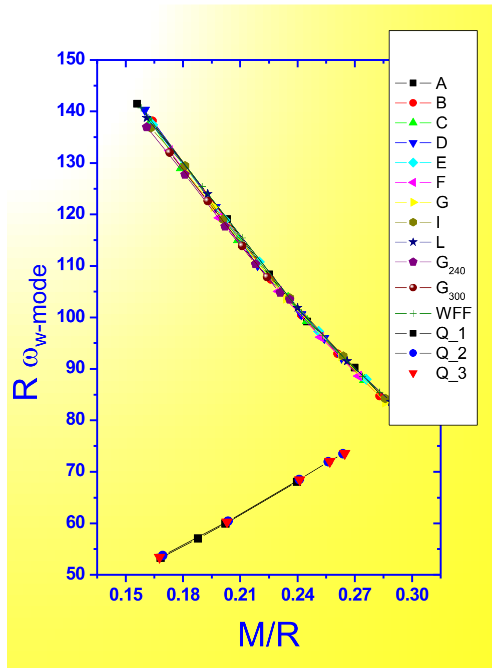

Andersson-KK 1996,-98, -01

Rotation "splits" the spectra

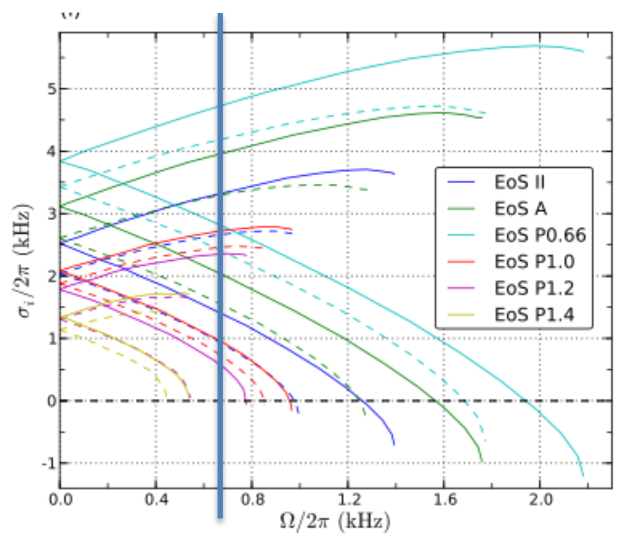

Gaertig-KK 2008

Finding order in chaos

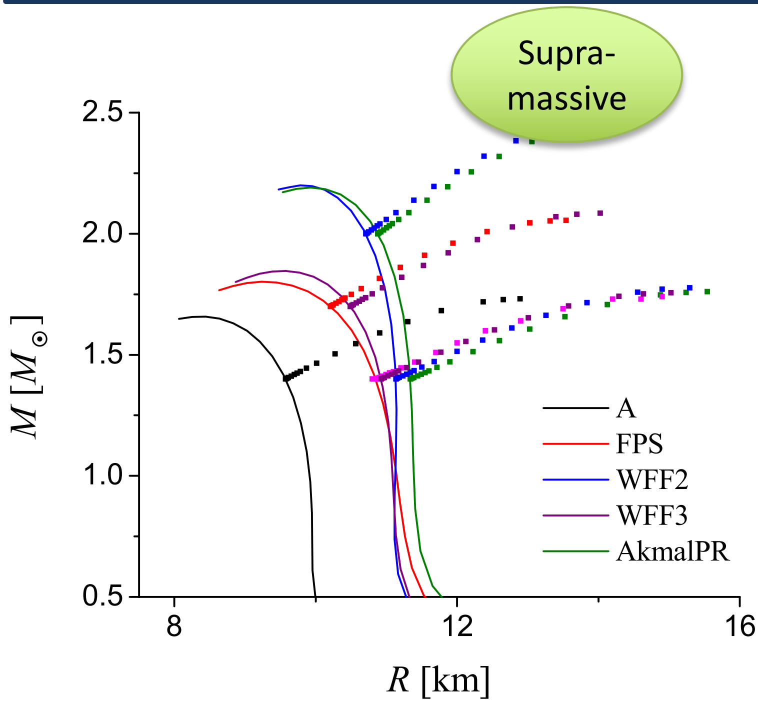

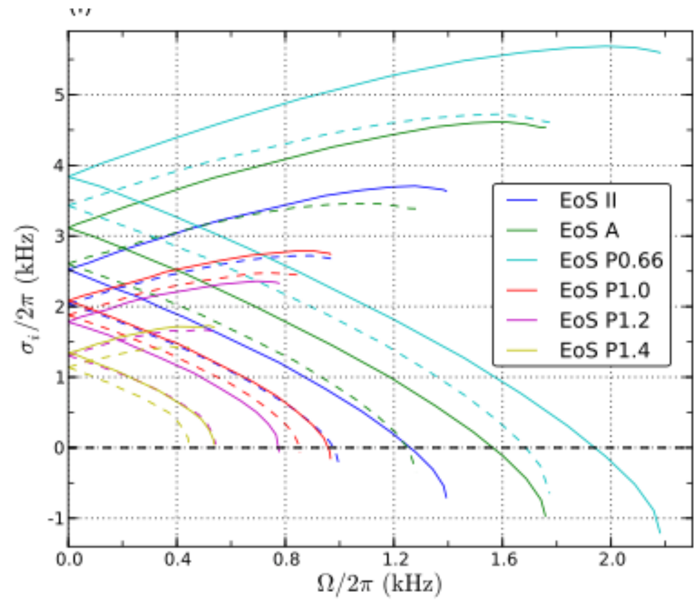

Reliable codes for the background

Perturbation equations
not manageable

Asteroseismology: f-modes
Cowling Approximation

Empirical relation connecting the parameters of the *rotating neutron stars* to the observed frequencies.

Frequency

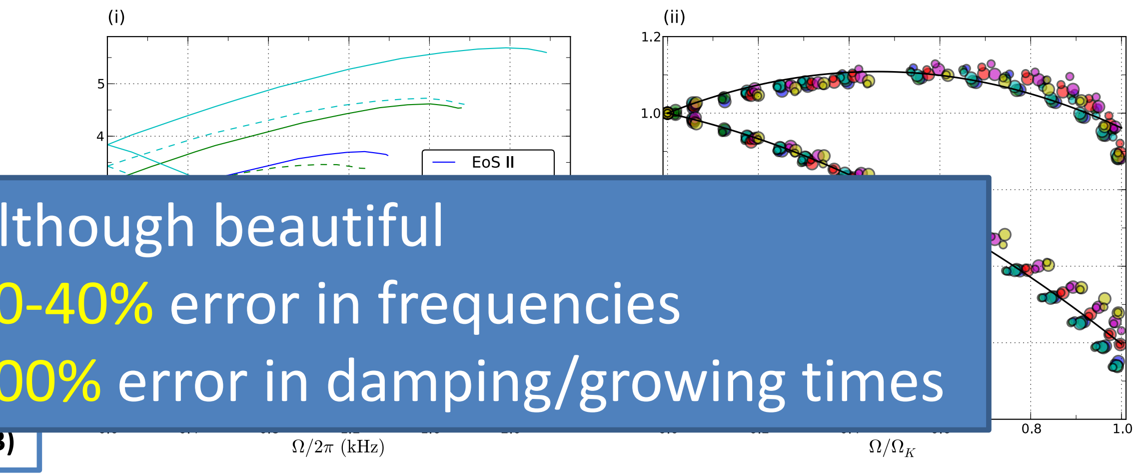

Although beautiful
20-40% error in frequencies
300% error in damping/growing times

Gaertig-Kokkotas 2008, 2010, 2011
Doneva, Gaertig, Kokkotas, Krüger (2013)

Damping/ Growth time

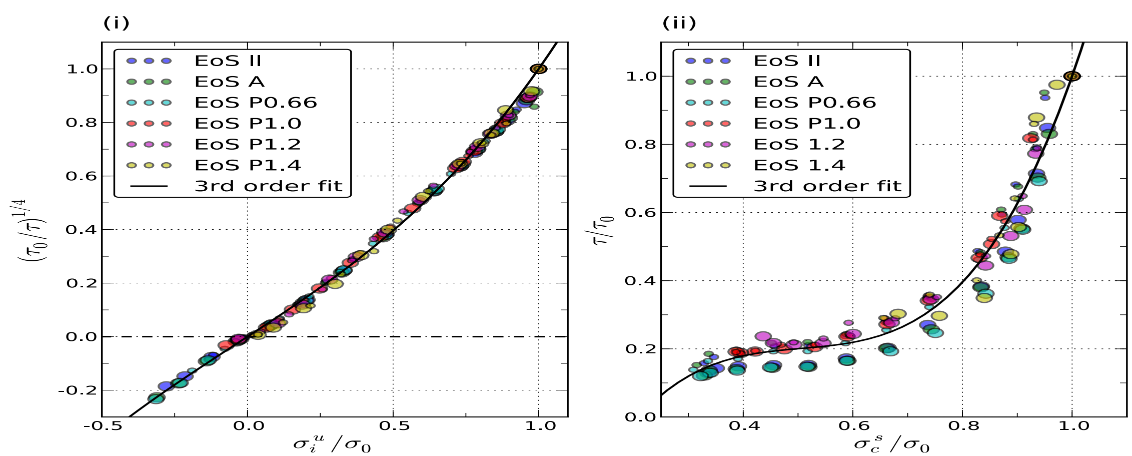

GW Asteroseismology: f-modes

$$M\sigma_i^{unst} = \left[(0.56 - 0.94\ell) + (0.08 - 0.19\ell)M\Omega + 1.2(\ell + 1)\eta\right]$$

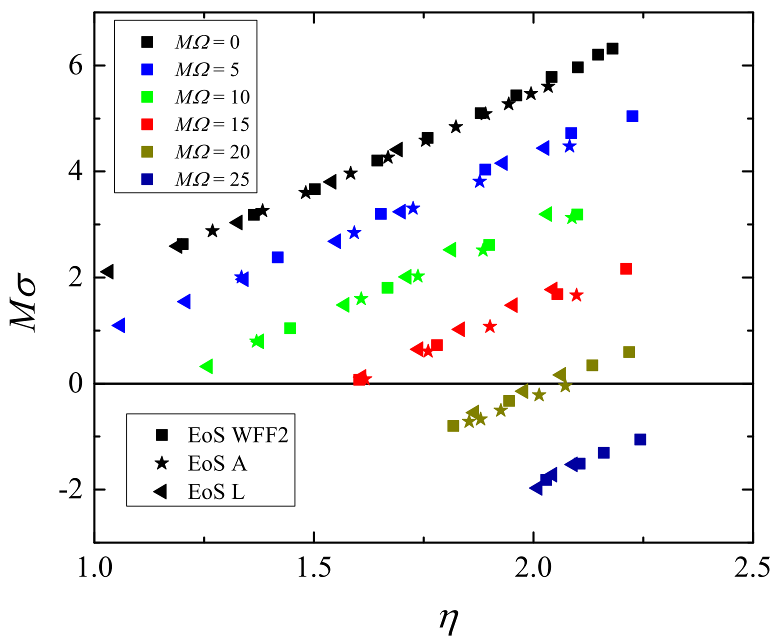

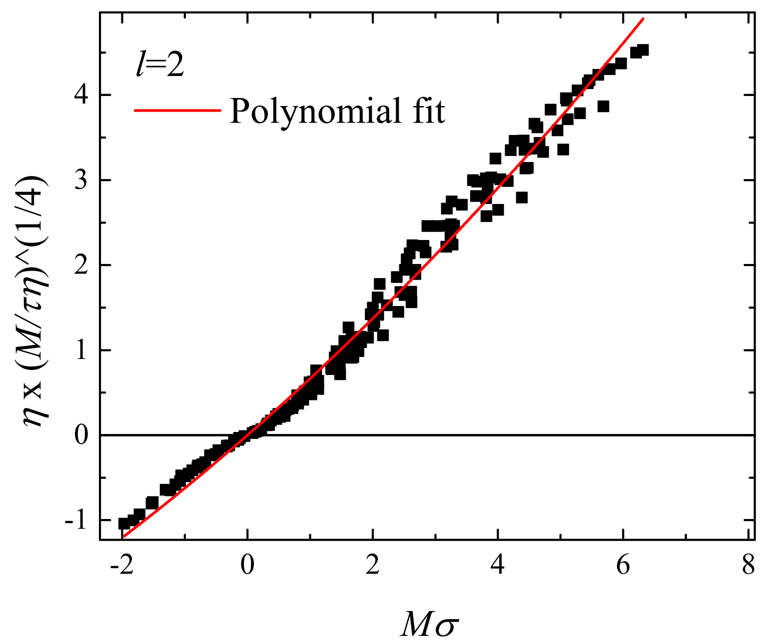

The ℓ = 2 f-mode oscillation frequencies and damping as functions of the parameter **η** (moment of inertia)

$$\eta = \sqrt{M^3 / I}$$

Doneva-Kokkotas 2015

Fast Rotating Neutron Star Perturbations
Basic Equations

Krüger-KK 2019

Equilibrium Configuration

$$ds^2 = -e^{2\nu}dt^2 + e^{2\psi}r^2\sin^2\theta(d\phi - \omega dt)^2 + e^{2\mu}(dr^2 + r^2 d\theta^2).$$

$$(u^t, u^r, u^\theta, u^\phi) = (u^t, 0, 0, \Omega u^t)\,.$$

$$T^{\mu\nu} = (\epsilon + p)u^\mu u^\nu + p g^{\mu\nu},$$

Perturbed Einstein Equations &
Conservation of Energy-Momentum

$$\begin{aligned} \delta G_{\mu\nu} &= 8\pi\delta T_{\mu\nu} \\ \delta\left(\nabla_\nu T^{\mu\nu}\right) &= 0. \end{aligned}$$

Choice of Gauge

$$\nabla^\nu h_{\mu\nu} = 0.$$

Hilbert/Lorenz

$$-2\delta G_{\mu\nu} = \nabla^\alpha\nabla_\alpha h_{\mu\nu} + 2R^\alpha{}_\mu{}^\beta{}_\nu h_{\alpha\beta} - R^\alpha_{[\mu} h_{\nu]\alpha} + R h_{\mu\nu} - g_{\mu\nu}R^{\alpha\beta}h_{\alpha\beta}.$$

Fast Rotating Neutron Star Perturbations
Basic Equations

Krüger-KK 2019

Due to axi-symmetry we can separate the azimuthal part of the perturbation

$$X(t,r,\theta,\phi) := \tilde{X}(t,r,\theta)e^{im\phi} \quad \Longrightarrow \quad \partial_\phi \to im$$

$\delta R_{tt} = 0$

$$\begin{aligned}
e^{2(\mu-\nu)}\partial_{tt}\mathcal{V}_1 &= \partial_{rr}\mathcal{V}_1 + \frac{1}{r^2}\partial_{\theta\theta}\mathcal{V}_1 \\
&+ \left(\nu_r + \psi_r + \frac{1}{r}\right)\partial_r\mathcal{V}_1 + \frac{1}{r^2}(\nu_\theta + \psi_\theta)\partial_\theta\mathcal{V}_1 + 2\left(\nu_r^2 + \frac{1}{r^2}\nu_\theta^2\right)\mathcal{V}_1
\end{aligned}$$

NOTE: These equations are for NON-ROTATING STARS !!!

$$\begin{aligned}
&+ 2\left[\mu_r\nu_r + \frac{1}{r}\nu_r - \frac{1}{r^2}\left(2\nu_\theta\psi_\theta + 2\nu_\theta^2 - \nu_{\theta\theta} - \mu_\theta\nu_\theta\right)\right]\mathcal{V}_3 - \frac{4}{r^2}\nu_\theta\partial_\theta\mathcal{V}_3 \\
&+ 2\left(\nu_r\psi_r + \frac{1}{r^2}\nu_\theta\psi_\theta\right)\mathcal{V}_4 \\
&+ \frac{1}{r^2}\left(\mu_r\nu_\theta + \nu_\theta\psi_r + \nu_{r\theta} + 2\nu_\theta\nu_r + \nu_r\psi_\theta + \mu_\theta\nu_r\right)\mathcal{Q} + \frac{1}{r^2}\nu_r\partial_\theta\mathcal{Q} + \frac{1}{r^2}\nu_\theta
\end{aligned}$$

+ 8 more for the spacetime
+ 4 for the fluid

$\delta R_{r\theta} = 0$

$$\begin{aligned}
e^{2(\mu-\nu)}\partial_{tt}\mathcal{Q} &= \partial_{rr}\mathcal{Q} + \frac{1}{r^2}\partial_{\theta\theta}\mathcal{Q} + \left(\psi_r + 3\nu_r - \frac{1}{r}\right)\partial_r\mathcal{Q} + \frac{1}{r^2}(3\nu_\theta + \psi_\theta)\partial_\theta\mathcal{Q} \\
&+ \left[2\nu_r\psi_r + 4\nu_r\mu_r - 4\mu_r^2 + \nu_r^2 - \psi_r^2 + 2\mu_{rr} + \frac{1}{r}(\nu_r - \psi_r - 6\mu_r) + \frac{1}{r^2}\left(-3 + 2\nu_\theta\psi_\theta + \nu_\theta^2 + 4\nu_\theta\mu_\theta - 4\mu_\theta^2 + 2\mu_{\theta\theta} - \psi_\theta^2\right)\right]\mathcal{Q} \\
&+ 8\left[2\nu_r\nu_\theta - \nu_\theta\mu_r - \mu_\theta\nu_r - \frac{1}{r}\nu_\theta + \nu_{r\theta}\right]\mathcal{V}_1 \\
&+ 8(\mu_\theta - \nu_\theta)\partial_r\mathcal{V}_2 - 8\left(\mu_r + \frac{1}{r}\right)\partial_\theta\mathcal{V}_2 + 4\left[\mu_\theta\psi_r + 3\mu_\theta\nu_r + \psi_r\psi_\theta - \nu_r\nu_\theta - \psi_\theta\mu_r - 2\nu_\theta\psi_r - 3\nu_\theta\mu_r - \frac{1}{r}(3\nu_\theta - \psi_\theta)\right]\mathcal{V}_2 \\
&+ 8\mu_\theta\partial_r\mathcal{V}_3 + 8\left(\mu_r - \nu_r + \frac{1}{r}\right)\partial_\theta\mathcal{V}_3 - 4\left[\mu_\theta\psi_r + 3\mu_\theta\nu_r - \psi_r\psi_\theta + \nu_r\nu_\theta - \psi_\theta\mu_r + \nu_r\psi_\theta - 3\nu_\theta\mu_r - \frac{1}{r}(3\nu_\theta - \psi_\theta)\right]\mathcal{V}_3 \\
&+ 8\left[\psi_{r\theta} - \mu_\theta\psi_r - \psi_\theta\mu_r + \nu_r\psi_\theta + \nu_\theta\psi_r - \frac{1}{r}\psi_\theta\right]\mathcal{V}_4
\end{aligned}$$

Fast Rotating Neutron Star Perturbations

Numerical Results

Krüger-KK 2019

A characteristic example

SPACETIME PERTURBATIONS
W-MODES

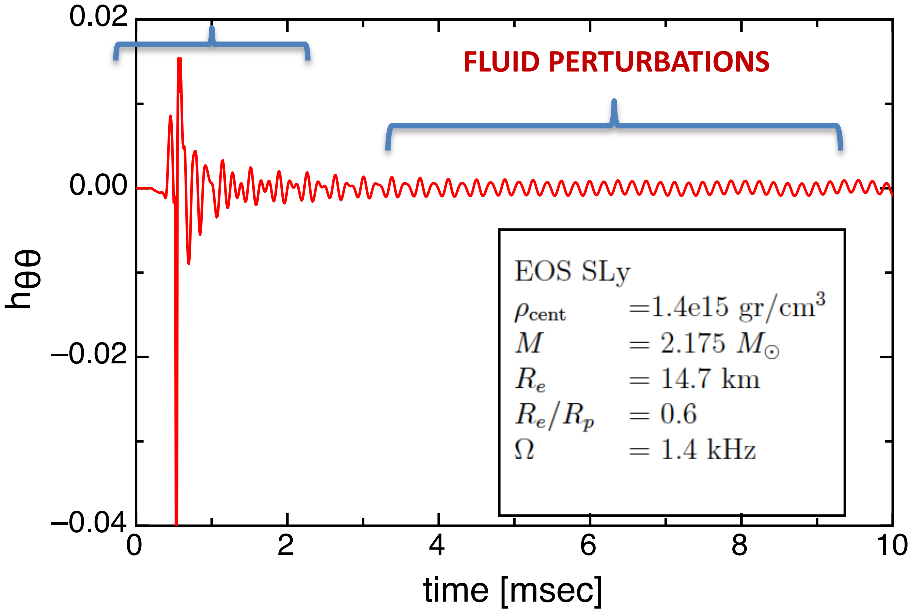

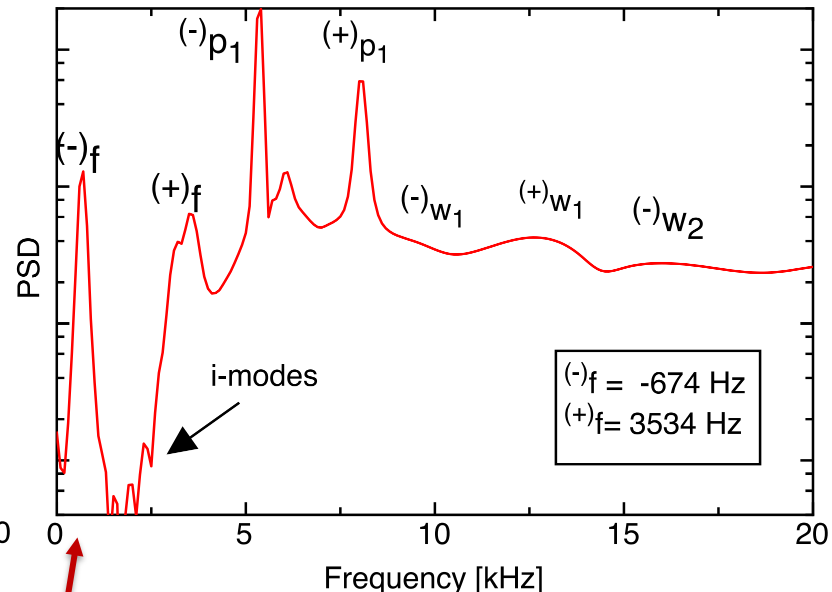

Ω/Ω_{Kepler} ~0.92

Unstable f-mode

Neutron Star Models

Fixed baryon mass & central density sequences

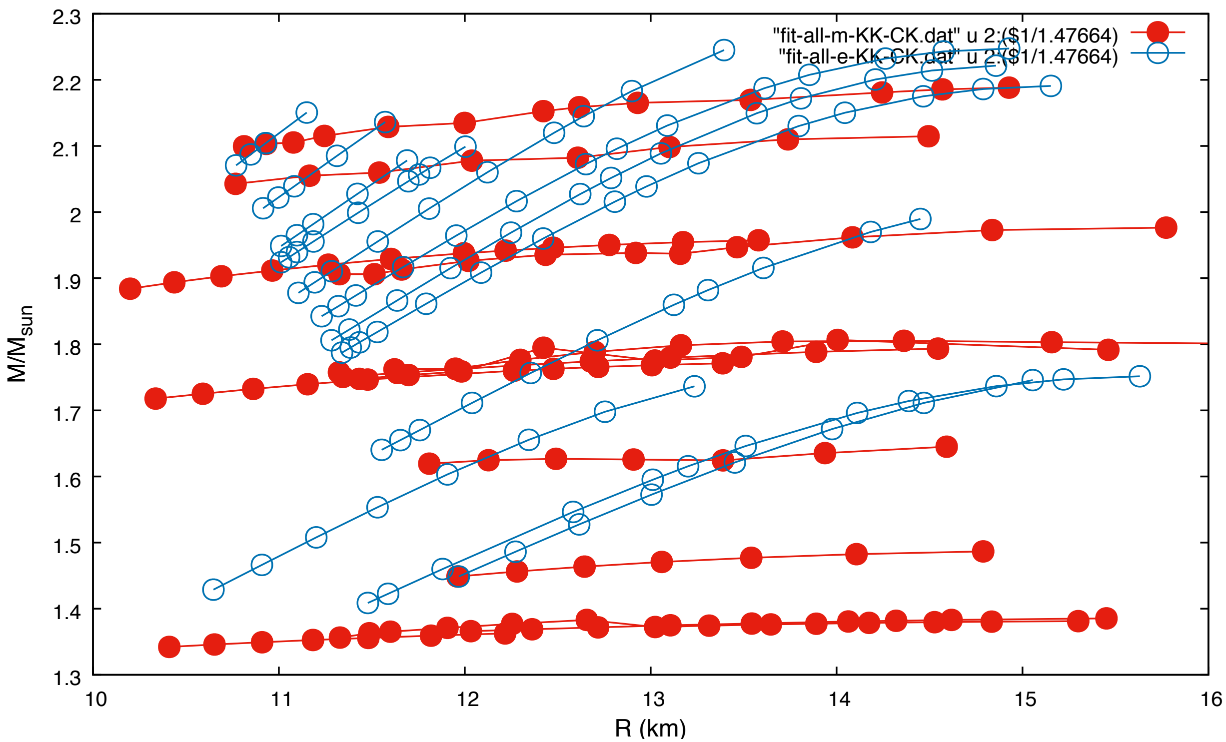

APR
3 – 39 fixed M_b
6 – 58 fixed ρ_c

SLy
7 – 65 fixed M_b
5 – 63 fixed ρ_c

WFF
3 – 28 fixed M_b
1 – 9 fixed ρ_c

Polytropes
5 – 52 fixed ρ_c

Krüger-KK 2019

Fitting Formulae

ω/ω_0 vs T/W

Krüger-KK 2019

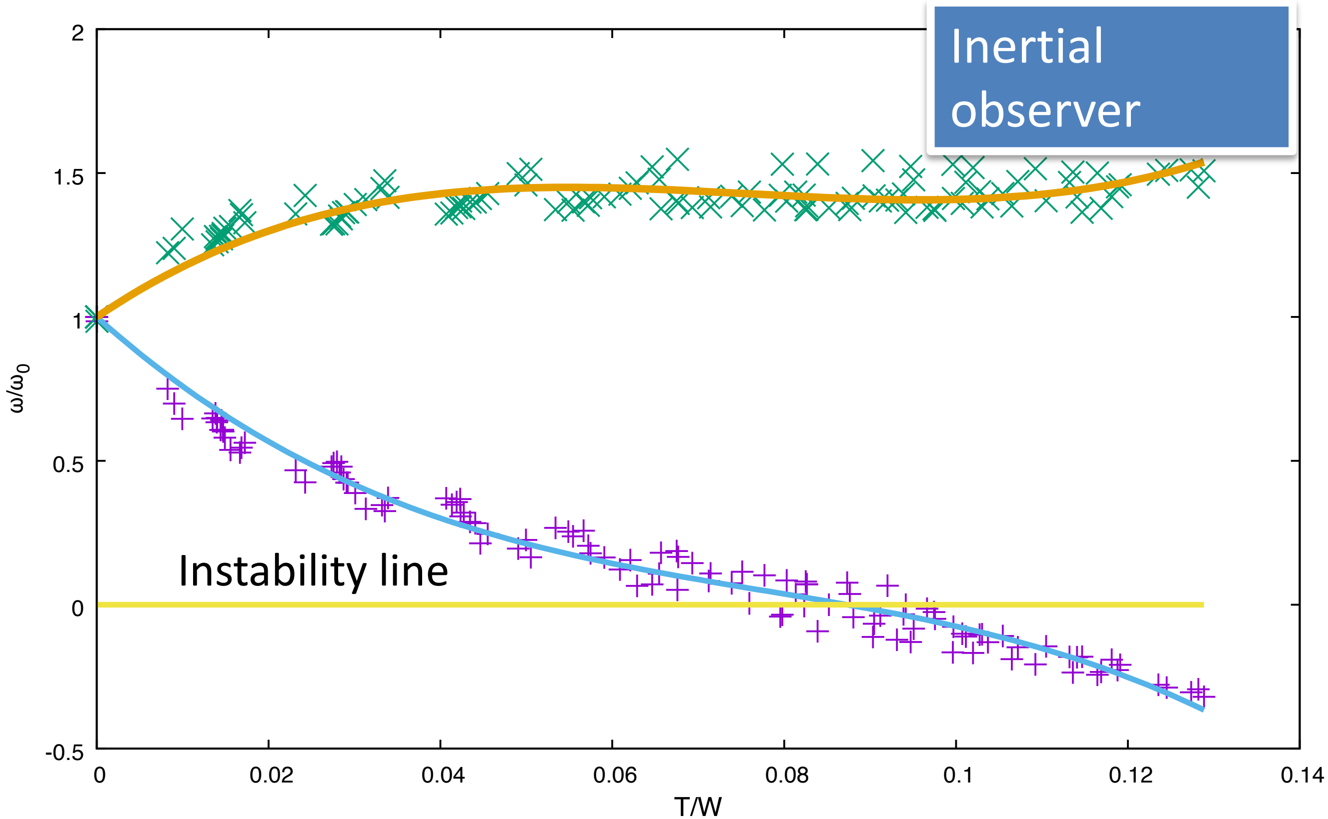

Fitting formula :

$$\left(\frac{\omega}{\omega_0}\right)_{\rm unst} = 1 - 27.8\left(\frac{T}{W}\right) + 301.8\left(\frac{T}{W}\right)^2 - 1324.4\left(\frac{T}{W}\right)^3$$

$$\left(\frac{\omega}{\omega_0}\right)_{\rm stab} = 1 + 21.9\left(\frac{T}{W}\right) - 313.7\left(\frac{T}{W}\right)^2 + 1408.9\left(\frac{T}{W}\right)^3$$

Similar for axis ratios

Fitting Formulae

ω/ω_0 vs T/W

Krüger-KK 2019

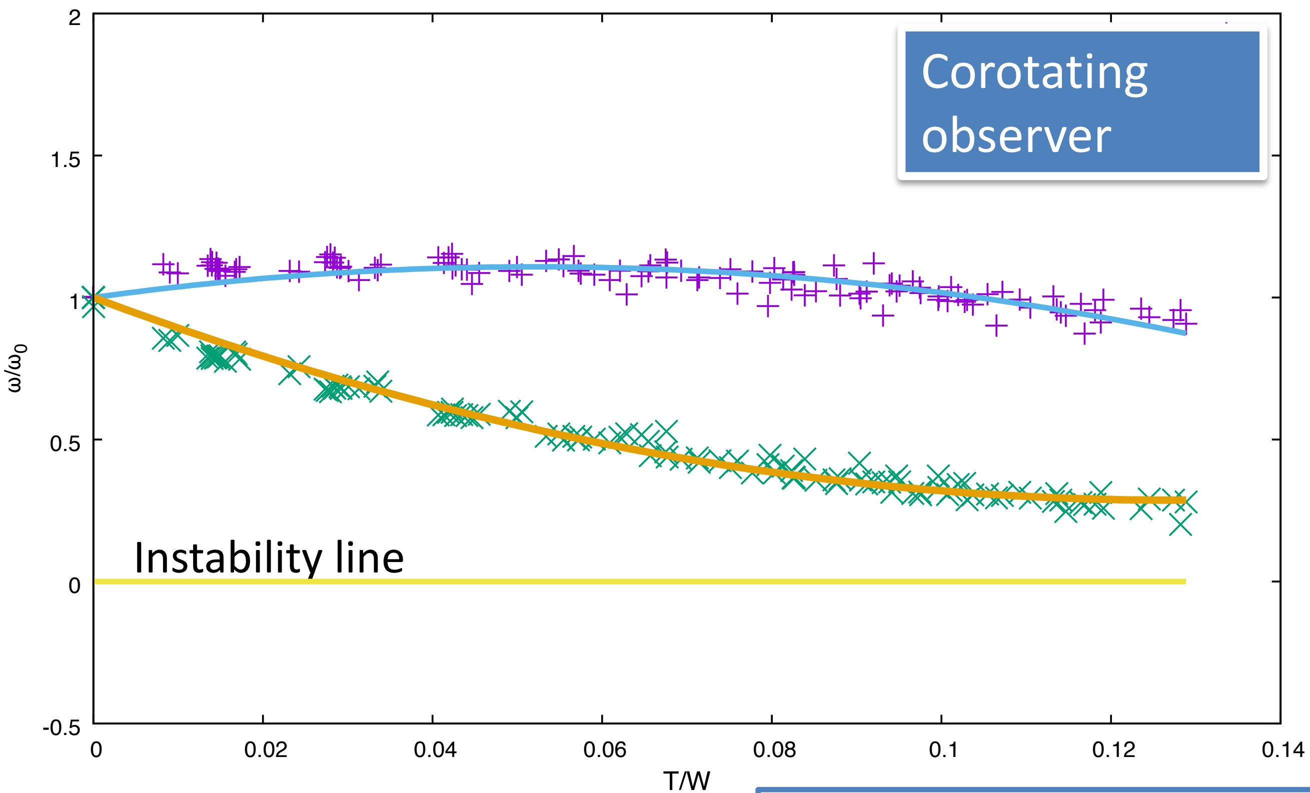

Fitting formula :

$$\left(\frac{\omega}{\omega_0}\right)^{\rm corot}_{\rm unst} = 1 + 4.15\left(\frac{T}{W}\right) - 39.8\left(\frac{T}{W}\right)^2$$

$$\left(\frac{\omega}{\omega_0}\right)^{\rm corot}_{\rm stab} = 1 - 11.2\left(\frac{T}{W}\right) + 43.9\left(\frac{T}{W}\right)^2$$

Similar for axis ratios

Fitting Formulae

ω/ω_0 vs Ω/ω_0

Krüger-KK 2019

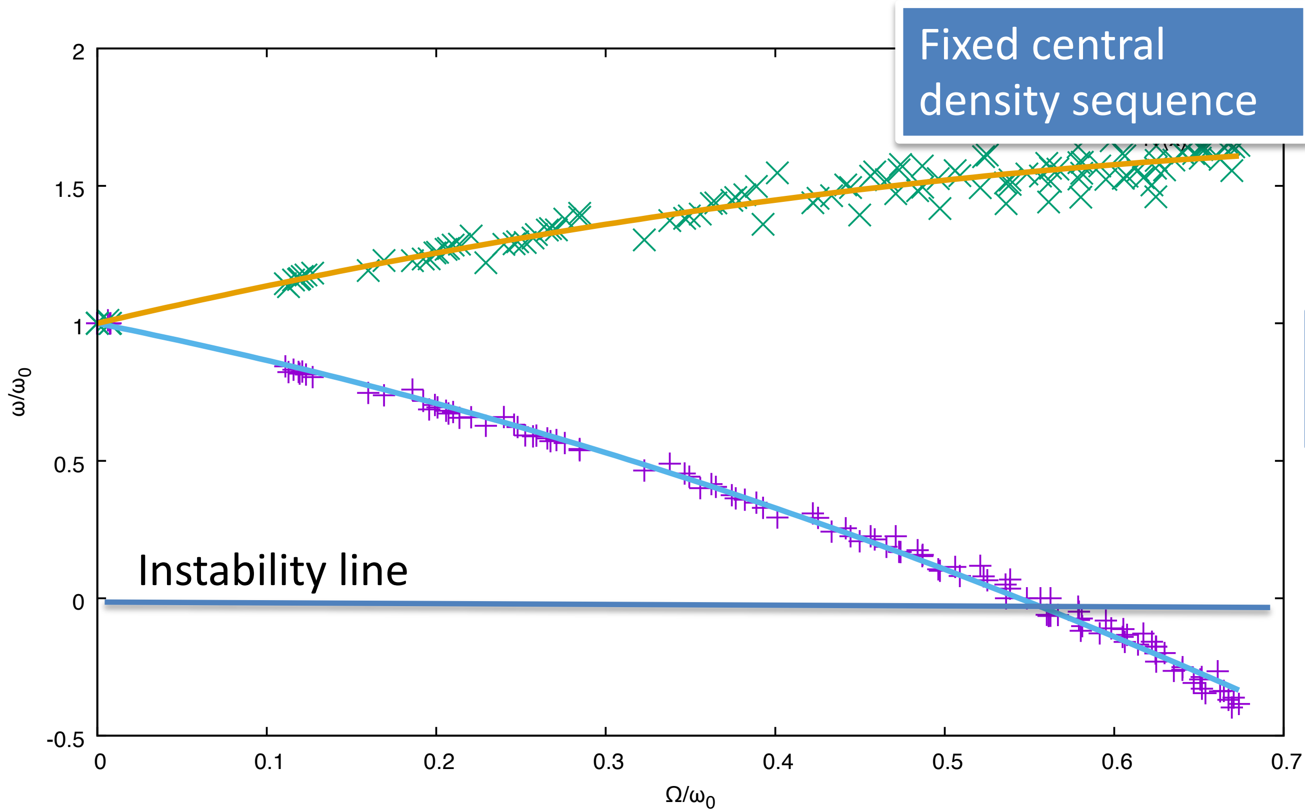

Typically **Ω_{Kepler}/ω_0~0.65**

Fitting formula :

$$\omega_0 \approx \alpha + \beta \left(M/R^3\right)^{1/2}$$

$$\left(\frac{\omega}{\omega_0}\right)_{\rm unst} = 1 - 1.24\left(\frac{\Omega}{\omega_0}\right) - 1.10\left(\frac{\Omega}{\omega_0}\right)^2$$

$$\left(\frac{\omega}{\omega_0}\right)_{\rm stab} = 1 + 1.44\left(\frac{\Omega}{\omega_0}\right) - 0.79\left(\frac{\Omega}{\omega_0}\right)^2$$

Fitting Formulae

$M\omega$ vs η

Krüger-KK 2019

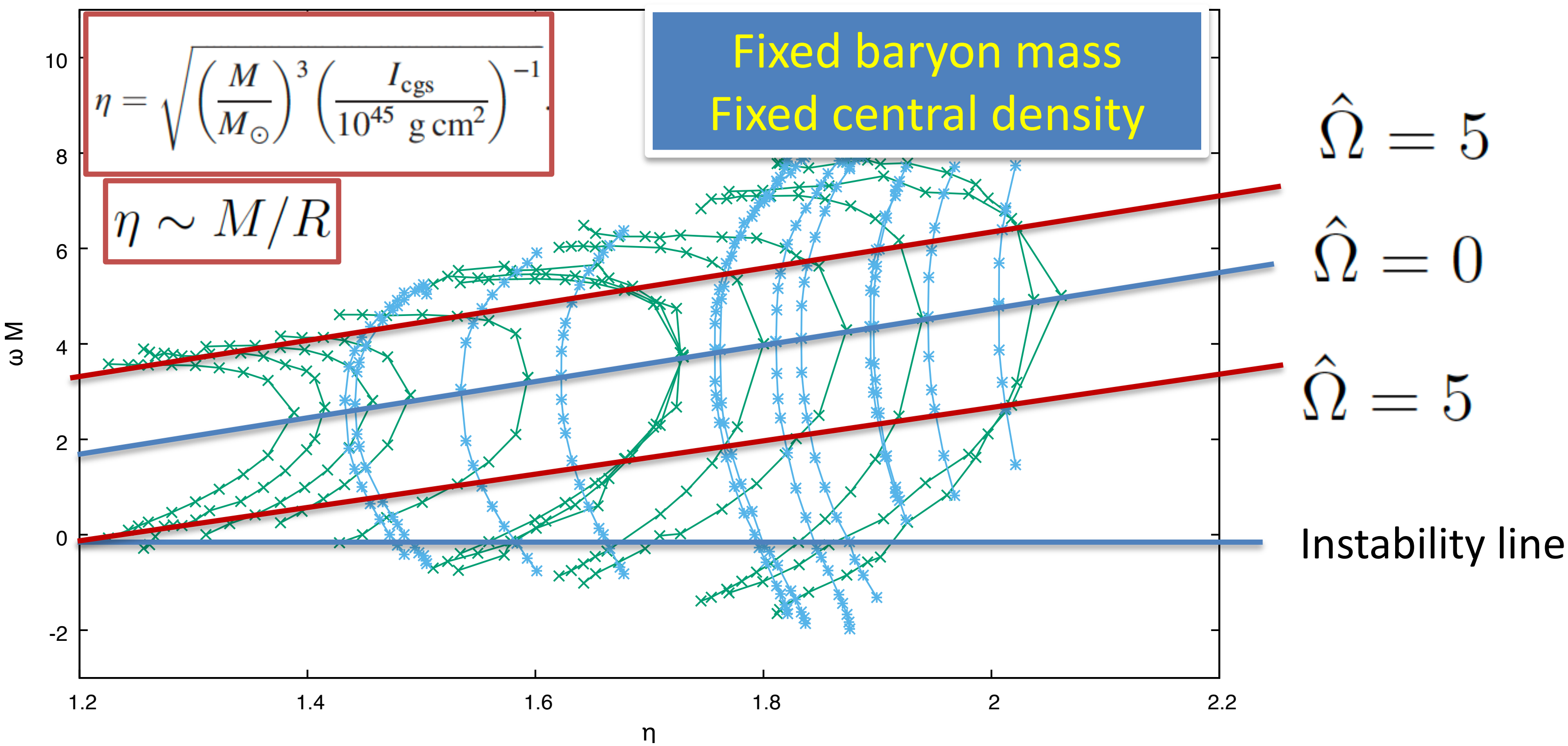

$$M\omega^{(+)} = \left(-2.38 + 0.43\hat{\Omega} - 5.07 \cdot 10^{-2}\hat{\Omega}^2\right) + \left(3.56 + 2.36 \cdot 10^{-2}\hat{\Omega}^2\right)\eta$$

$$M\omega^{(-)} = \left(-2.38 - 0.41\hat{\Omega} - 2.89 \cdot 10^{-3}\hat{\Omega}^2\right) + \left(3.56 + 7.88 \cdot 10^{-3}\hat{\Omega}^2\right)\eta$$

$$\hat{\Omega} = M\Omega$$

Non-rotating case: Tsui-Leung 2005

Lattimer-Schutz 2005 : I vs M/R

For the Cowling case: Doneva+Kokkotas 2015

Binary Neutron Star Mergers

Early: Post-merger Oscillations & GWs

GRAVITATIONAL WAVES

NEUTRON STAR OSCILLATIONS

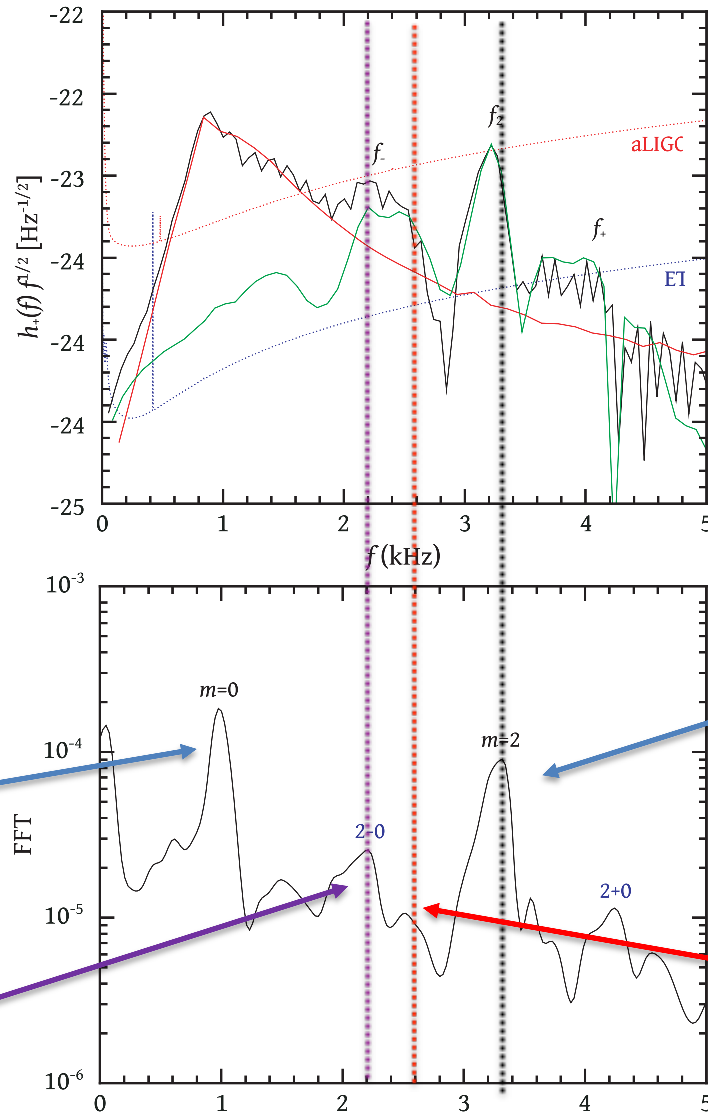

Stergioulas et al. (2011)
Bauswein, Stergioulas (2015)
...
Krüger, Kokkotas (2019)

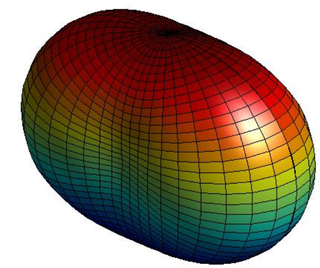

l=m=2
linear f-mode (f_{peak})

l=m=0 linear quasi-radial mode

Quasi-linear combination frequency (f_{2-0})

nonlinear spiral frequency

Oscillations & Instabilities
In the GW Era

- **Collapse**
  - Torres-Forné, A. et. al (2018, 19) – exitation of f, g-modes.
  - Westernacher-Schneider J. R, et.al (2019)
- **Pre-Merger Phase** (Love number)
  - Wen, De-Hua et.al (2019)
  - Rosofsky, Shawn G. etal (2019)
  - Andersson, Pnigouras (2019)
  - Chakravarti, Andersson (2019)
  - Schmidt, Hinderer (2019)
- **Early post-Merger phase**
  - Bauswein,Stergioulas, Janka 2015-2019
- **Late post-Merger phase**
  - Doneva, KK, Pnigouras (2015)

Binary Neutron Star Mergers
LATE post-merger phase

Formation of a “stable” NS

Slowdown due to three competing mechanisms:

I. Typical dipole B-field spindown

$$t_{sd} \approx 7 \left(\frac{B_d}{10^{15} G} \right)^{-2} \left(\frac{P}{1ms} \right)^{2} hr$$

II. Deformed Magnetar Model

Dall’Osso-Giacomazzo-Perna-Stella 2015

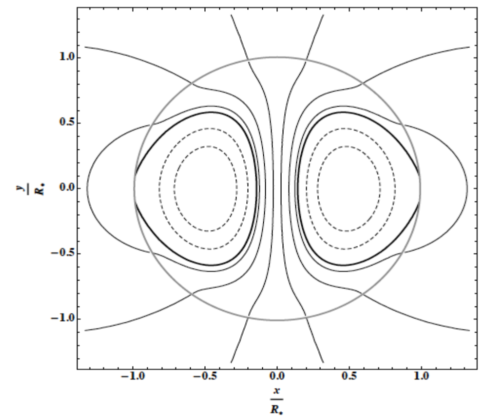

III. Rotational Instabilities

Doneva-Kokkotas-Pnigouras 2015

$l = 2, m = 2$

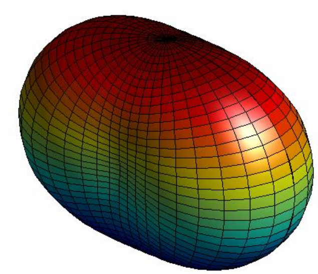

Post-Merger NS:
F-mode instability vs Magnetic field

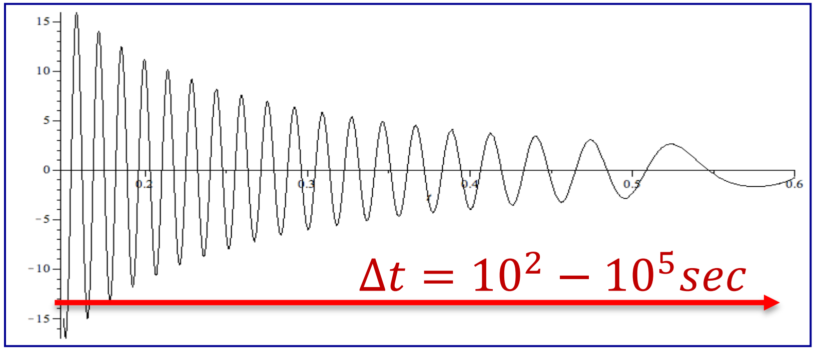

Competition between the B-field and the secular instability

GW frequencies:
WW2a: 920-1000 Hz
APR: 370–810 Hz
WFF2b: 600–780 Hz

Doneva-Kokkotas-Pnigouras 2015

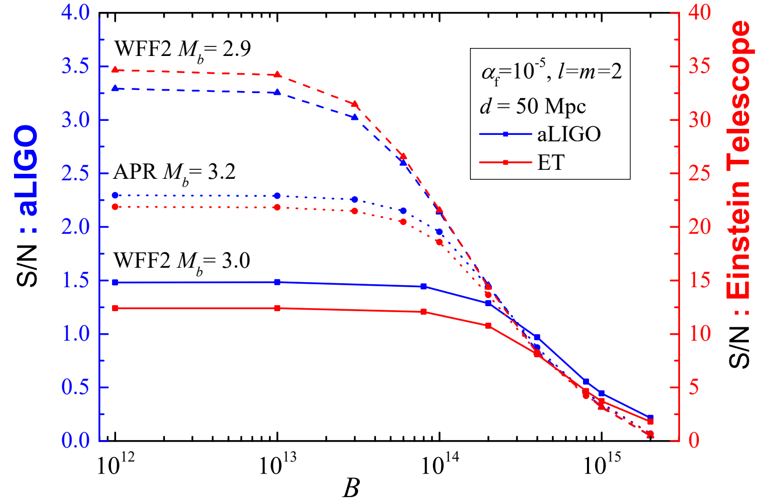

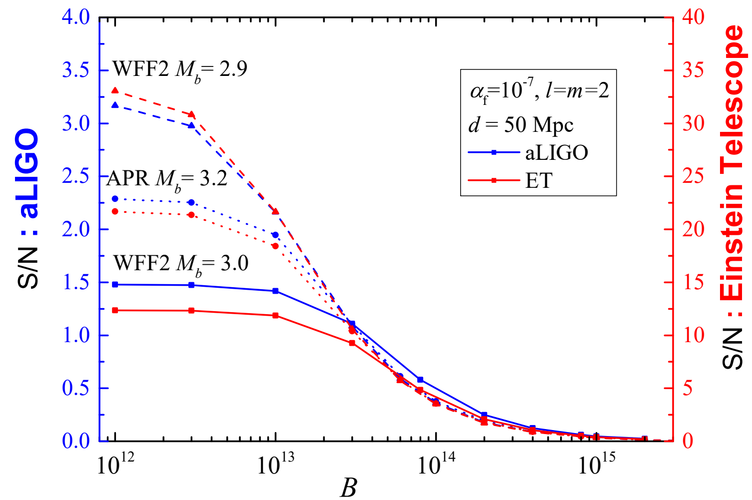

EBERHARD KARLS UNIVERSITÄT TÜBINGEN

Inverse Problem in the Spectra of Compact Object

Kostas Kokkotas & **Sebastian Völkel**

Theoretical Astrophysics, University of Tübingen

90s: An interesting observation by Chandrasekhar-Ferrari

1991: A reconsideration of the axial modes

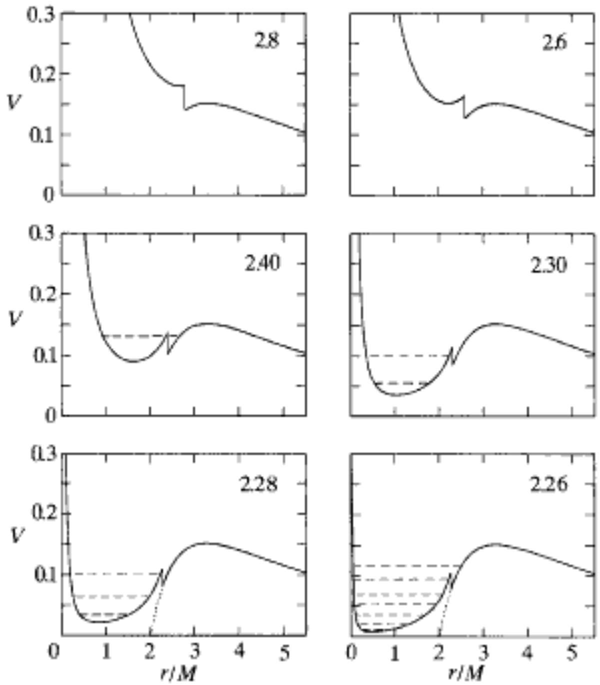

CF 1991

$$X_{,r,r} - \frac{2}{ry}\left(1 - 2\epsilon r^2 \frac{y_1}{3y_1 - y}\right) X_{,r} - \frac{(l-1)(l+2)}{r^2 y} X + \frac{4\sigma^2}{y(3y_1 - y)^2} X = 0,$$

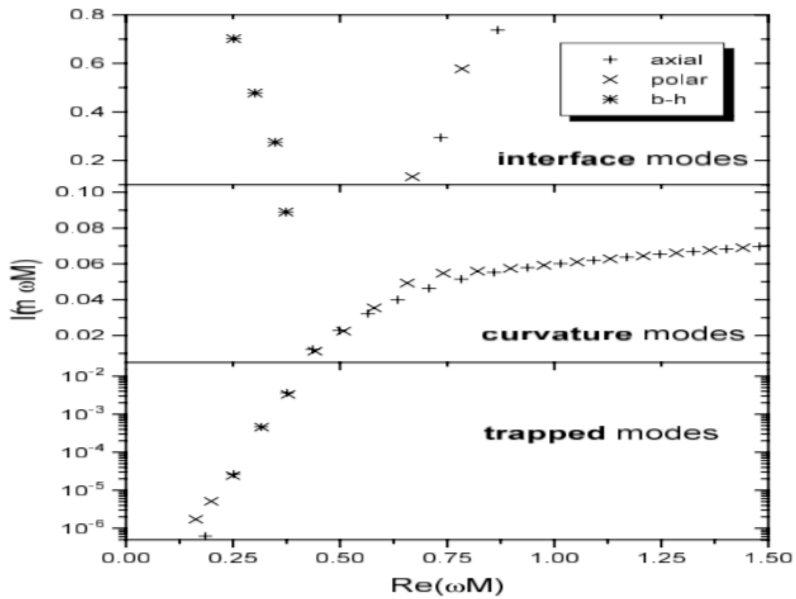

KK 1995

An interesting observation by Chandrasekhar-Ferrari

1991: A reconsideration of the axial modes

$$V(r) = \left(1 - \frac{2M}{r}\right)\left[\frac{l(l+1)}{r^2} - \frac{6M}{r^3}\right]$$ Black-Holes

$$\frac{d^2}{dr^{*2}}\Psi(r) + \left(\omega_n^2 - V(r)\right)\Psi(r) = 0,$$

$$V(r) = \frac{e^{2\nu}}{r^3}\left[l(l+1)r + r^3(\rho - p(r)) - 6M(r)\right]$$

Axial oscillations of stars

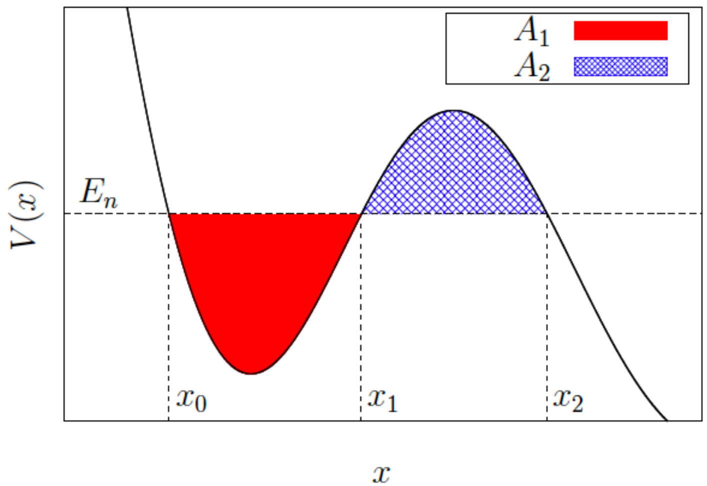

Völkel-Kokkotas 2017

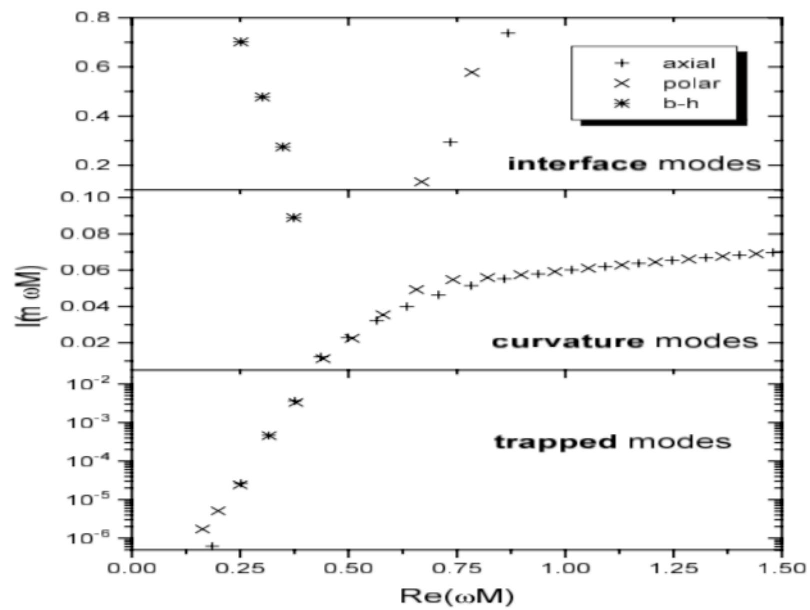

Kokkotas 1995

An interesting “toy” problem

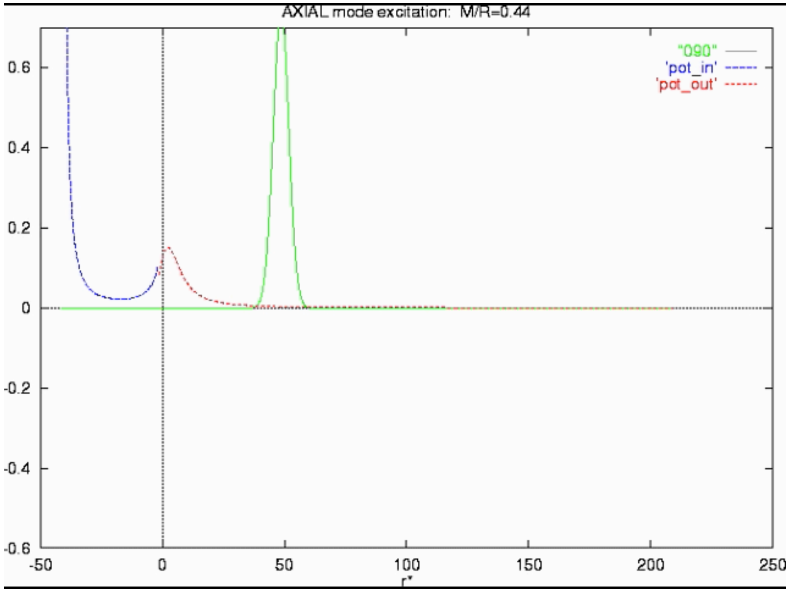

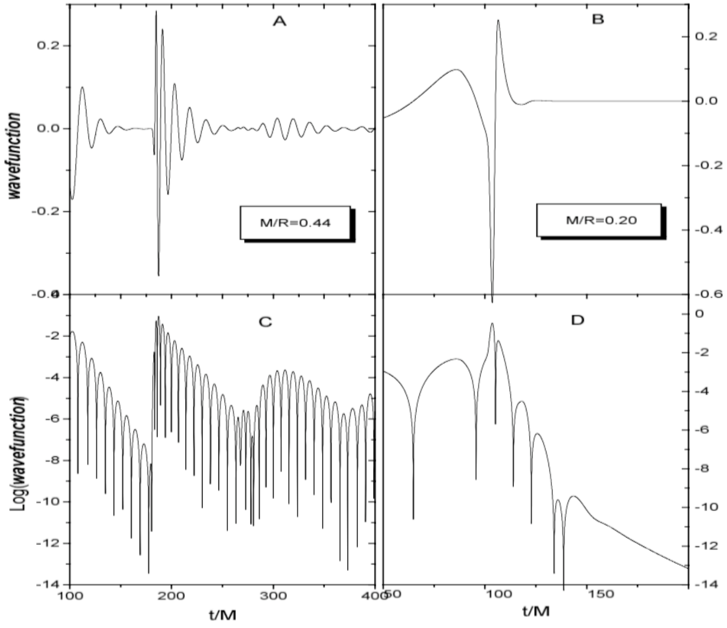

KK: Les Houches 1995

W-mode or Ergoregion Instability

- Perturbations of the spacetime, similar to the QNMs of BHs (Kokkotas+Schutz 1986-1992)
- Frequencies (typical) 5-12kHz
- Damping times (typical) ≥0.1ms
- For very compact stars they become exciting! (Chandrasekhar+Ferrari 1991)

- The creation of an ergosphere signals the onset of an instability (Friedman 1978, Comins+Schutz 1978)
- The dragging is so strong that any timelike backwards moving trajectory gets dragged forward

- Growth time of the order of tenths of secs
- It sets in quite early for very compact NS ($R/M \sim 2.26$, $\Omega \sim 0.19 \Omega_{Kepler}$)

Kokkotas-Ruoff-Andersson 2004

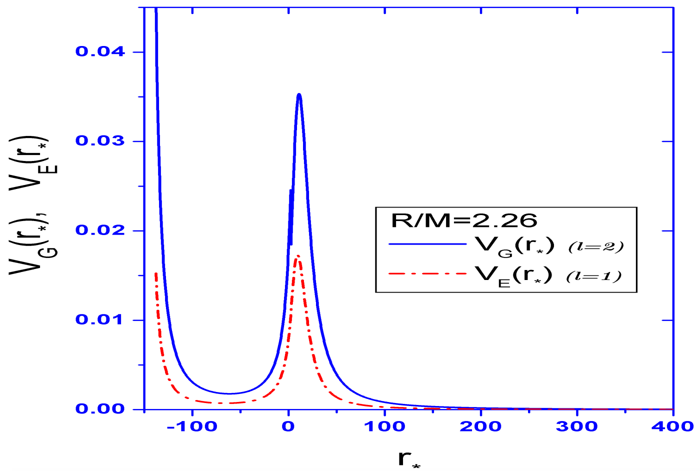

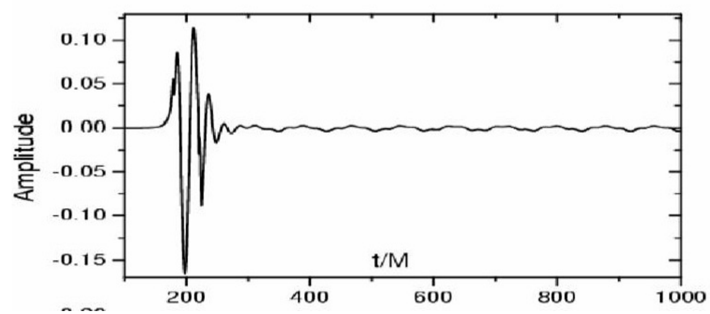

- No direct way for viscosity to suppress the instability (!)
- Nonlinear saturation (?)

Different types of axial perturbation potentials

$$\frac{\mathrm{d}^2}{\mathrm{d}r^{*2}}\Psi(r) + \left(\omega_n^2 - V(r)\right)\Psi(r) = 0,$$

$$V(r) = \frac{e^{2\nu}}{r^3}\left[l(l+1)r + r^3(\rho - p(r)) - 6M(r)\right]$$

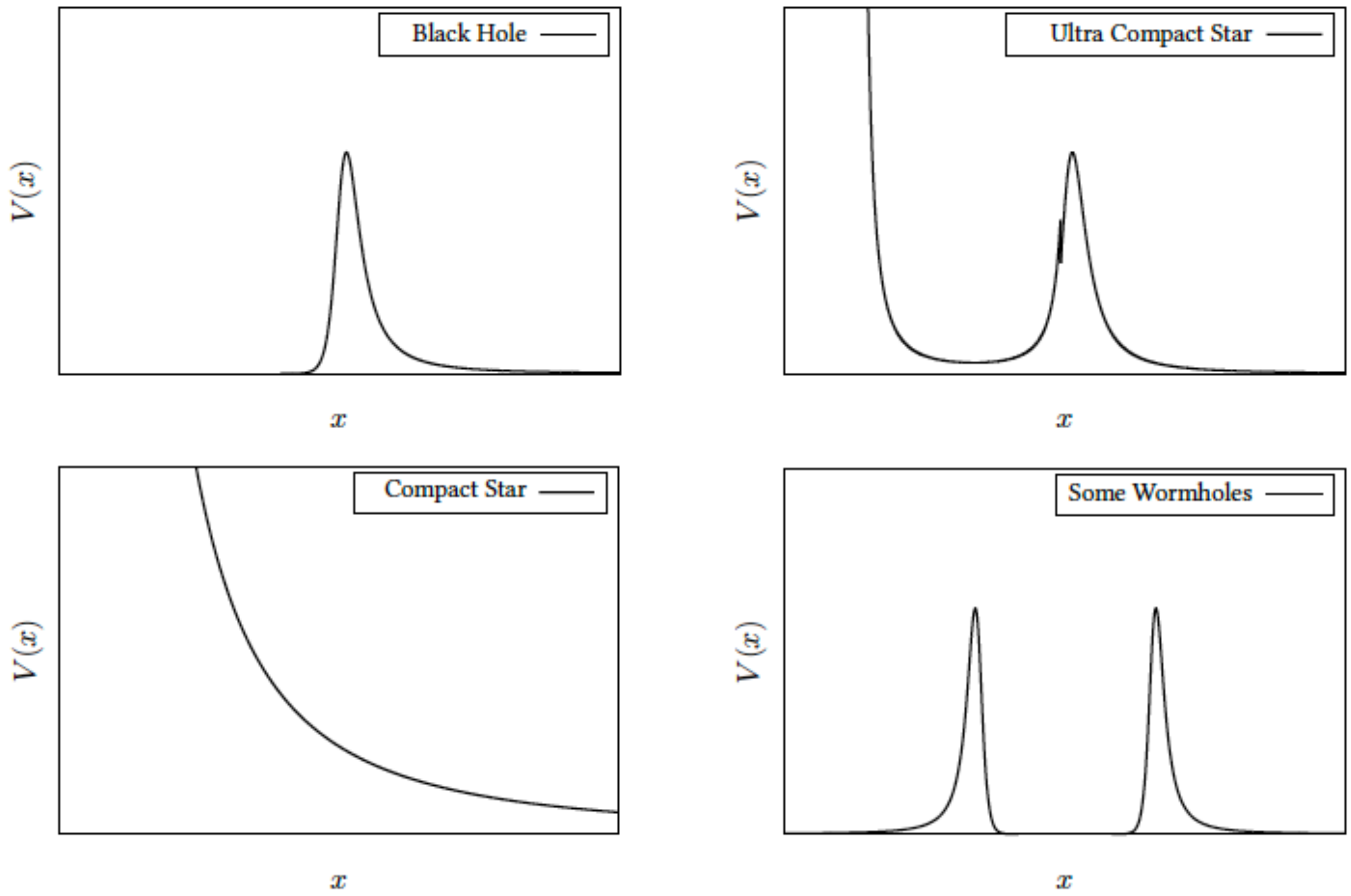

Different types of axial spectra

$$\frac{d^2}{dr^{*2}}\Psi(r) + \left(\omega_n^2 - V(r)\right)\Psi(r) = 0, \qquad V(r) = \frac{e^{2\nu}}{r^3}\left[l(l+1)r + \boxed{r^3(\rho - p(r))} - 6M(r)\right]$$

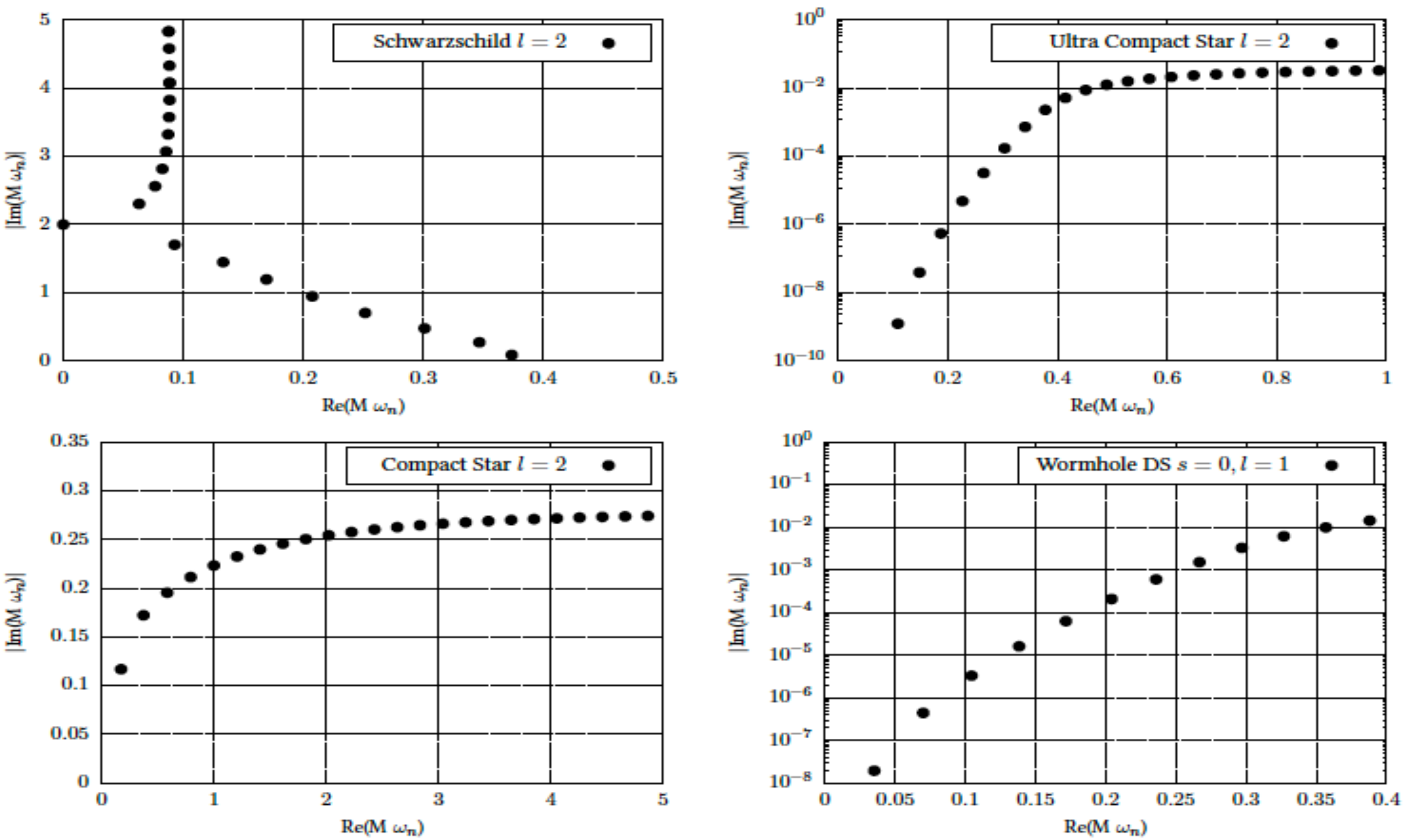

Axial spectra & Echoes

$$\frac{d^2}{dr^{*2}}\Psi(r) + \left(\omega_n^2 - V(r)\right)\Psi(r) = 0,$$

$$V(r) = \frac{e^{2\nu}}{r^3}\left[l(l+1)r + r^3(\rho - p(r)) - 6M(r)\right]$$

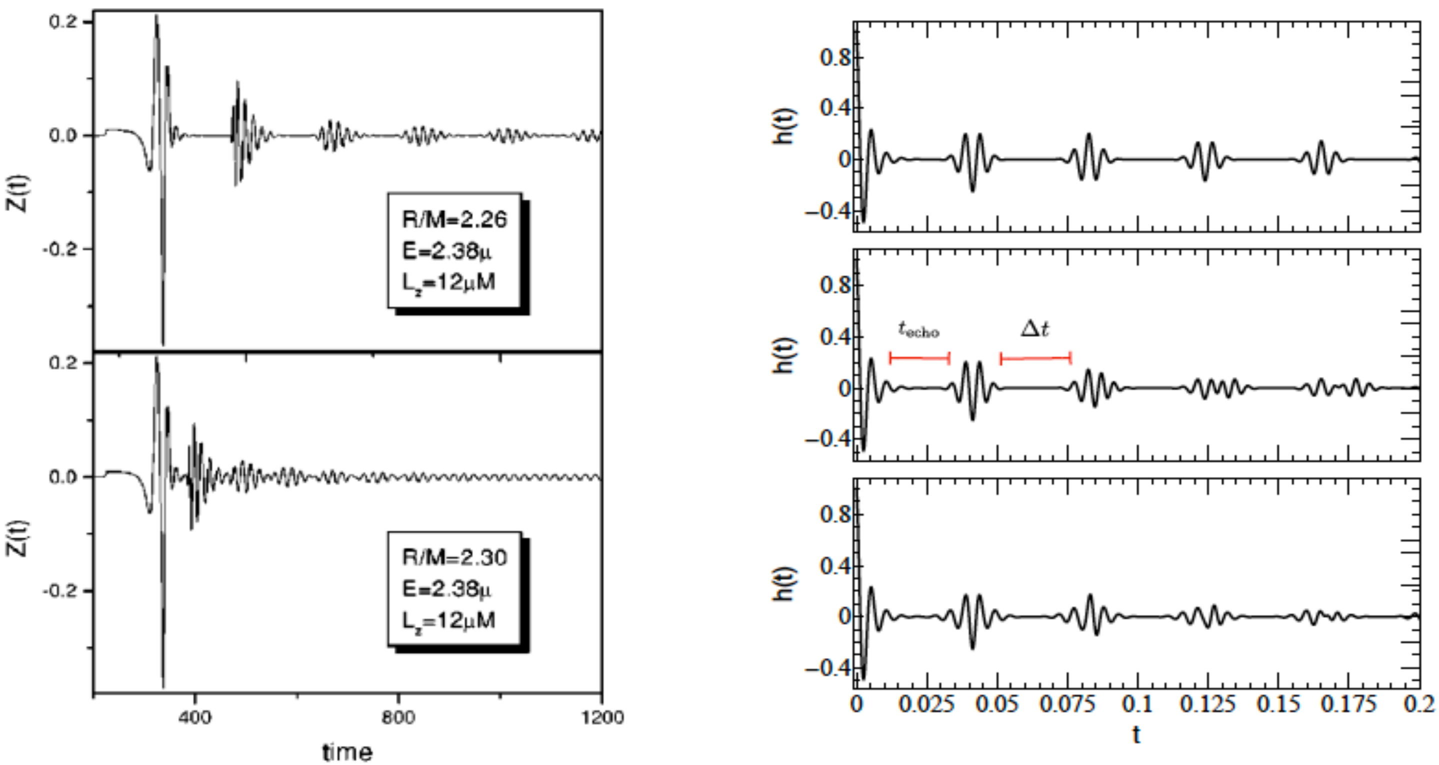

Figure 2: Left: Axial perturbations ultra compact stars, Ferrari & Kokkotas (2000). Right: Phenomenological template for parameter estimation: Maselli, Völkel & Kokkotas (2018).

Different types of calculation methods

$$\frac{d^2}{dr^{*2}}\Psi(r) + \left(\omega_n^2 - V(r)\right)\Psi(r) = 0, \qquad V(r) = \frac{e^{2\nu}}{r^3}\left[l(l+1)r + \boxed{r^3(\rho - p(r))} - 6M(r)\right]$$

- Methods for **direct** QNM calculations:
  Continued fraction, Green's functions, Time-evolution,. . .

- But, **reconstructing** potential/properties of the source from the spectrum is different (uniqueness?)

- **WKB** method and **Bohr-Sommerfeld** rules[4] are powerful here (approximate, but easier to invert)

$$\int_{x_0}^{x_1}\sqrt{E_n - V(x)}\mathrm{d}x = \pi\left(n + \frac{1}{2}\right) - \frac{i}{4}\exp\left(2i\int_{x_1}^{x_2}\sqrt{E_n - V(x)}\mathrm{d}x\right) \quad (2)$$

[4] here $E_n \equiv \omega_n^2$

Inversion Method for Different types of potentials

$$\frac{d^2}{dr^{*2}}\Psi(r) + \left(\omega_n^2 - V(r)\right)\Psi(r) = 0,$$

$$V(r) = \frac{e^{2\nu}}{r^3}\left[l(l+1)r + \boxed{r^3(\rho - p(r))} - 6M(r)\right]$$

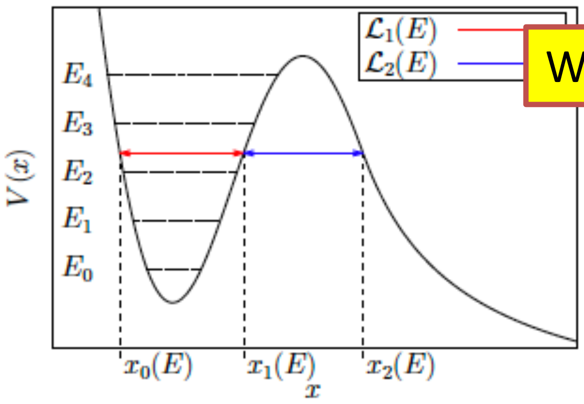

Wheeler 1976

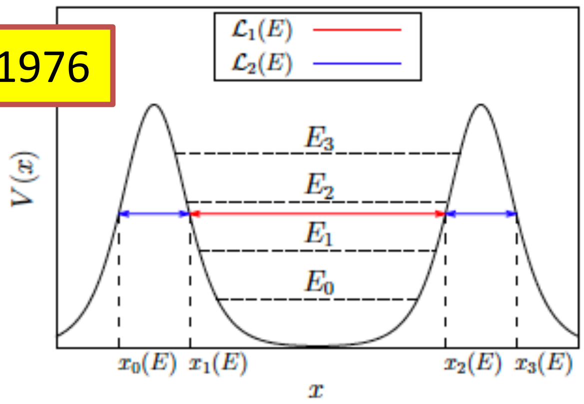

Figure 3: Völkel & Kokkotas (2017)

Figure 4: Völkel & Kokkotas, (2018)

$$\mathcal{L}_1(E) = x_1 - x_0 = 2\frac{\partial}{\partial E}\int_{E_{\min}}^{E}\frac{n(E') + 1/2}{\sqrt{E - E'}}\mathbf{d}E'$$

$$\mathcal{L}_2(E) = x_2 - x_1 = -\frac{1}{\pi}\int_{E}^{E_{\max}}\frac{(\mathbf{d}T(E')/\mathbf{d}E')}{T(E')\sqrt{E' - E}}\mathbf{d}E'$$

Inversion Method for stellar potentials

$$\frac{\mathrm{d}^2}{\mathrm{d}r^{*2}}\Psi(r) + \left(\omega_n^2 - V(r)\right)\Psi(r) = 0,$$

$$V(r) = \frac{e^{2\nu}}{r^3}\left[l(l+1)r + \boxed{r^3(\rho - p(r))} - 6M(r)\right]$$

Example for ultra compact constant density star $C \approx 0.44$

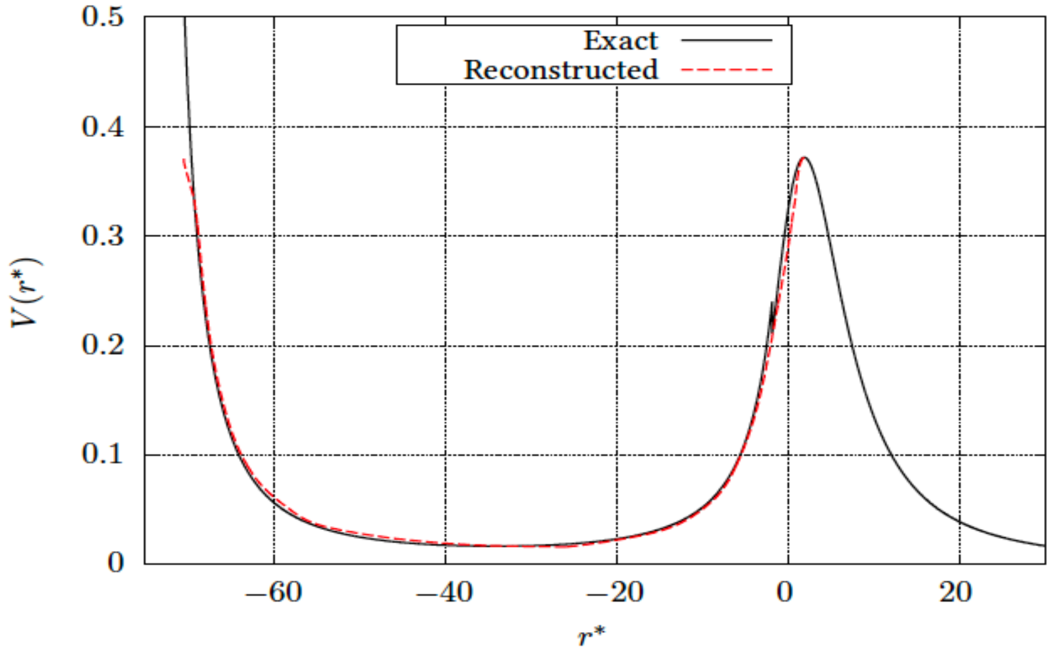

Reconstructed axial perturbation potential, constant density star, $l = 3$, taken from Völkel and Kokkotas (2017,2).

Inversion Method for DS wormhole

$$\frac{\mathrm{d}^2}{\mathrm{d}r^{*2}}\Psi(r) + \left(\omega_n^2 - V(r)\right)\Psi(r) = 0,$$

$$V(r) = \frac{e^{2\nu}}{r^3}\left[l(l+1)r + r^3(\rho - p(r)) - 6M(r)\right]$$

Example for Damour-Solodukhin wormhole $C \approx 0.5$

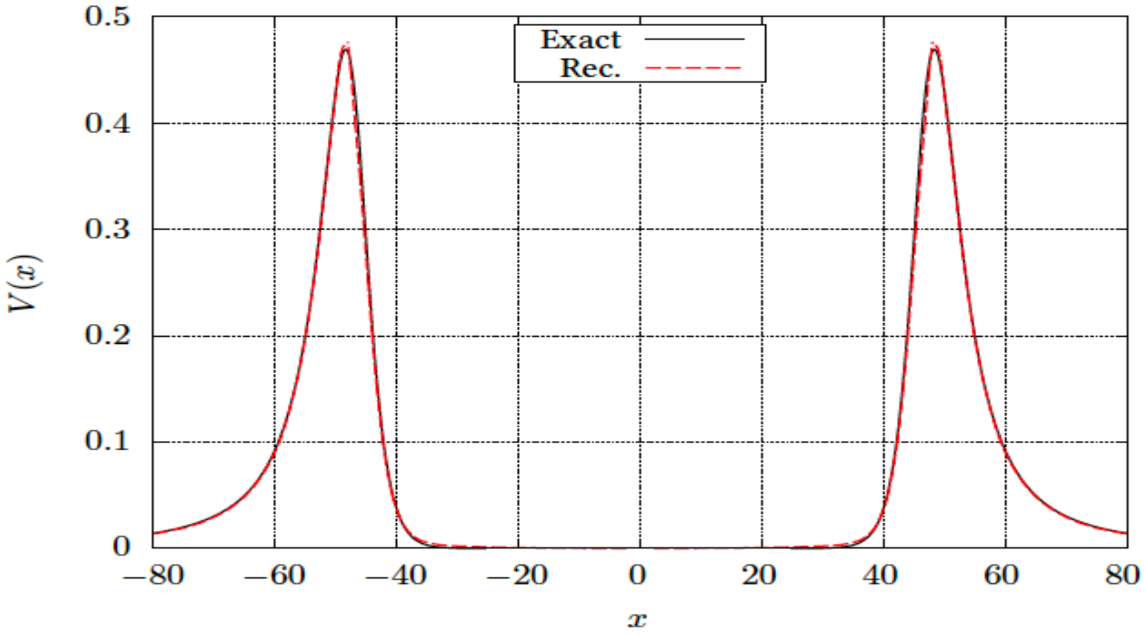

Reconstructed scalar perturbation potential, Damour-Solodukhin wormhole, $l = 3$, taken from Völkel and Kokkotas (2018,2).

Inversion Method for normal NS

$$\frac{\mathrm{d}^2}{\mathrm{d}r^{*2}}\Psi(r) + \left(\omega_n^2 - V(r)\right)\Psi(r) = 0,$$

$$V(r) = \frac{e^{2\nu}}{r^3}\left[l(l+1)r + r^3(\rho - p(r)) - 6M(r)\right]$$

Example for neutron star polytrope $C \approx 0.15$

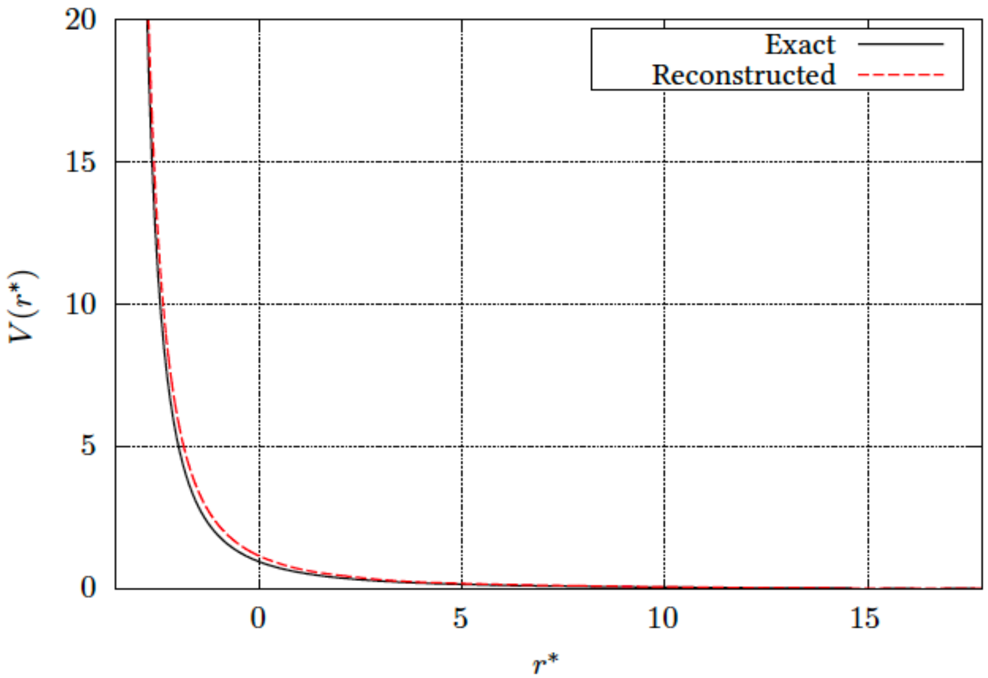

Reconstructed axial perturbation potential, neutron star polytrope, $l = 3$, Völkel and Kokkotas (2019) .

Inversion Problem for Hawking Radiation

Völkel, Konoplya, Kokkotas PRD 2019

Assuming Hawking radiation can be described by

$$\frac{\mathrm{d}E}{\mathrm{d}t} = \sum_{l} N_l \left|\mathcal{A}_l\right|^2 \frac{\omega}{\exp\left(\omega / T_{\mathrm{H}}\right) - 1} \frac{\mathrm{d}\omega}{2\pi},$$

T_H Hawking temperature, $\mathcal{A}_l$ greybody factors, N_l multiplicities [4]

$$\begin{aligned} \Psi &= e^{-i\omega r_*} + R e^{i\omega r_*}, \quad & r_* \to +\infty, \\ \Psi &= T e^{-i\omega r_*}, & r_* \to -\infty, \end{aligned}$$

reflection R and transmission T

$$\left|\mathcal{A}_\ell\right|^2 = 1 - \left|R_\ell\right|^2 = \left|T_\ell\right|^2.$$

[4] Details in Kanti, Kodama, Konoplya, Pappas, and Zhdenko (2009)

Inversion Problem for Hawking Radiation

Völkel, Konoplya, Kokkotas PRD 2019

Analytic approximation given by Gamow formula

$$T(E) = \exp\left(2i\int_{x_0}^{x_1}\sqrt{E - V(x)}\mathrm{d}x\right), \qquad (5)$$

E energy, $V(x)$ potential barrier, and x_0 and x_1 classical turning points[5].

Can be inverted to find width of potential barrier[6]

$$\mathcal{L}(E) \equiv x_1 - x_0 = \frac{1}{\pi}\int_{E}^{E_{\max}} \frac{(\mathrm{d}T(E')/\mathrm{d}E')}{T(E')\sqrt{E' - E}}\mathrm{d}E', \qquad (6)$$

But, how do we get the individual greybody factors?

[5] Defined by $E = V(x)$

[6] Cole & Good PRA (1978)

Inversion Problem for Hawking Radiation

Völkel, Konoplya, Kokkotas PRD 2019

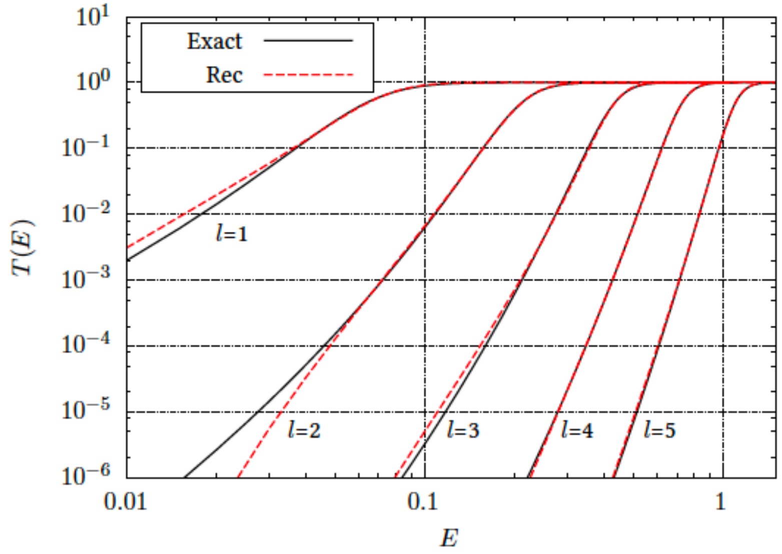

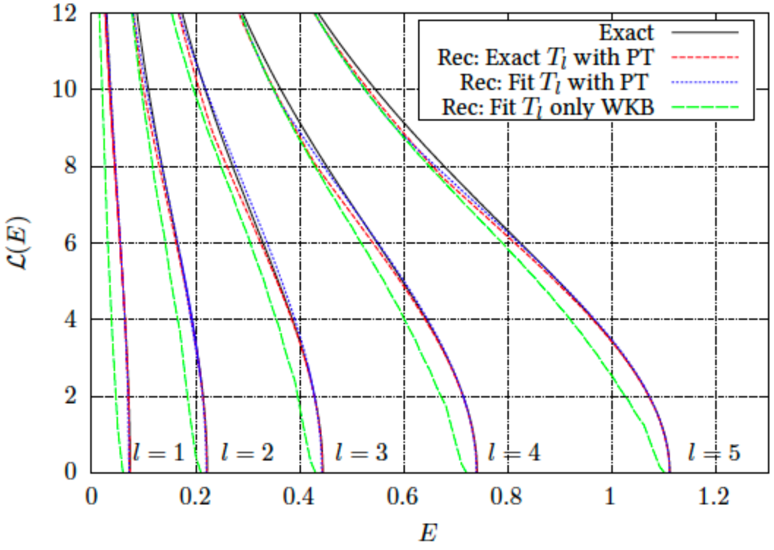

Reconstruction of the **Schwarzschild transmissions** $T_l(E)$ from Hawking spectrum fitting

Reconstruction of the **Schwarzschild potential barrier** widths $\mathbf{L_l(E)}$ from given transmissions $T_l(E)$.

Inversion Problem for Hawking Radiation

Völkel, Konoplya, Kokkotas PRD 2019

For black hole QNMs, Schutz-Will formula (1985) based on parabolic potential approximation, easily gives fundamental modes, but fails for overtones.

Hawking radiation involves **summation** over several greybody factors

Parabolic approximation yields

$$T_l(E) = \left(1 + \exp\left(-\frac{\pi\left(E - V_{\mathrm{max},l}\right)}{\sqrt{a_l}}\right)\right)^{-1}, \qquad (7)$$

$T_l(E)$ has non-trivial contribution only around $V_{\mathrm{max},l}$.

For smaller or larger energies, $T_l(E)$ is either 0 or 1, respectively

$$V_{\mathrm{max},l} \equiv V_{\mathrm{BH}}(r^*_{\mathrm{max},l}), \qquad a_l \equiv -\frac{V''_{\mathrm{max},l}}{2}. \qquad (8)$$

Inversion Problem for Hawking Radiation

Völkel, Konoplya, Kokkotas PRD 2019

$$\mathcal{I}(E) \equiv \sum_l N_l |\mathcal{A}_l|^2 \equiv \sum_l I_l(E).$$

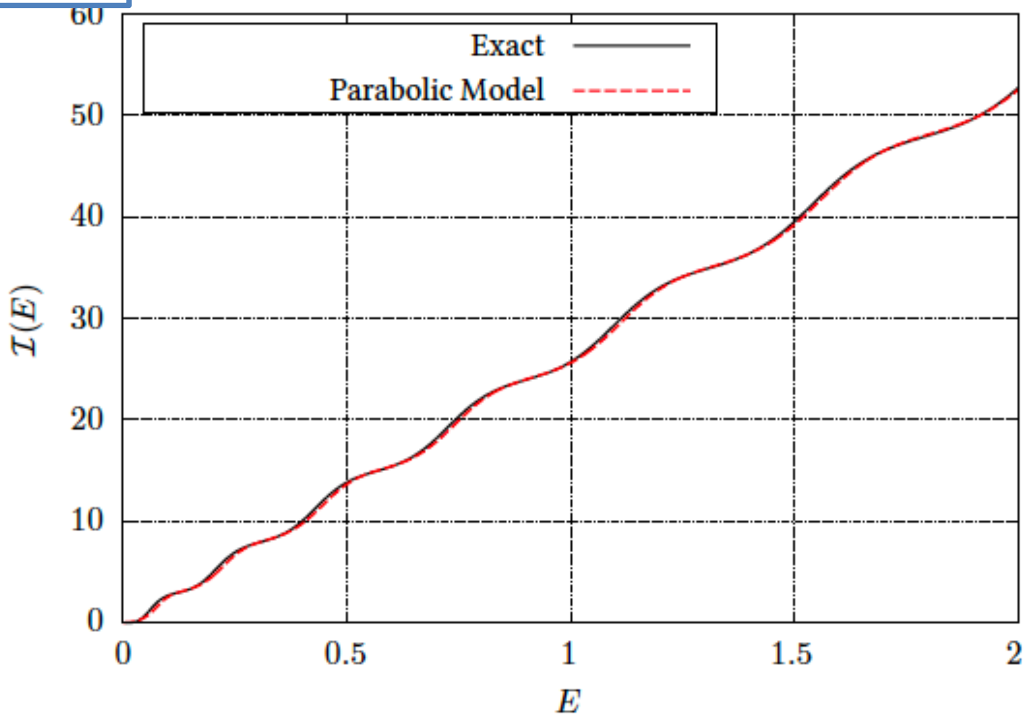

Comparison of the exact result (black solid) and parabolic approximation (red dashed) for the normalized energy emission spectrum of the Schwarzschild black hole.

THANK YOU